



Measurement of the c -jet mistagging efficiency in $t\bar{t}$ events using pp collision data at $\sqrt{s} = 13$ TeV collected with the ATLAS detector

ATLAS Collaboration*

CERN, 1211 Geneva 23, Switzerland

Received: 23 September 2021 / Accepted: 17 November 2021
© CERN for the benefit of the ATLAS collaboration 2022

Abstract A technique is presented to measure the efficiency with which c -jets are mistagged as b -jets (mistagging efficiency) using $t\bar{t}$ events, where one of the W bosons decays into an electron or muon and a neutrino and the other decays into a quark–antiquark pair. The measurement utilises the relatively large and known $W \rightarrow cs$ branching ratio, which allows a measurement to be made in an inclusive c -jet sample. The data sample used was collected by the ATLAS detector at $\sqrt{s} = 13$ TeV and corresponds to an integrated luminosity of 139 fb^{-1} . Events are reconstructed using a kinematic likelihood technique which selects the mapping between jets and $t\bar{t}$ decay products that yields the highest likelihood value. The distribution of the b -tagging discriminant for jets from the hadronic W decays in data is compared with that in simulation to extract the mistagging efficiency as a function of jet transverse momentum. The total uncertainties are in the range 3–17%. The measurements generally agree with those in simulation but there are some differences in the region corresponding to the most stringent b -jet tagging requirement.

1 Introduction

The algorithms for the identification of jets containing b -hadrons, also known as b -tagging algorithms, constitute an important tool for the analysis of the data collected by the ATLAS experiment [1] at the Large Hadron Collider (LHC) [2]. Such algorithms play a crucial role in a large number of Standard Model (SM) precision measurements (e.g. Refs. [3,4]), Higgs boson measurements (e.g. Refs. [5,6]), and searches for supersymmetry and other exotic phenomena (e.g. Refs. [7,8]).

The performance of the b -tagging algorithms depends crucially on whether the jets that are identified contain b -hadrons (b -jets), c -hadrons (c -jets), or neither of them (light-flavour jets). The Monte Carlo (MC) simulation provides an esti-

mate of the probability that a jet fulfils the requirements of the b -tagging algorithm i.e. the tagging efficiency for b -jets and the mistagging efficiency for c -jets and light-flavour jets. However, since the simulation is not perfect, the (mis)tagging efficiency must be measured in data. Simulation to data scale factors (SFs), which are defined as the ratio of the efficiency measured in data to that in simulation, are used as a correction to the simulation, assuming that the SFs are independent of the physics process. Analyses that use b -tagging apply a weight to each simulated event, derived as the product of the SFs for all jets for which a tagging requirement is made.

Measurements of the SFs have been made using $t\bar{t}$ events for b -jets [9,10] and inclusive jet events for light-flavour jets [11]. Measurements of SFs for c -jets using proton–proton (pp) collision data at $\sqrt{s} = 7$ TeV, described in Ref. [12], use two methods to measure the mistagging efficiency of c -jets. One technique uses the production of a W boson in association with a c -jet that decays semi-muonically and the other identifies a D^* meson within c -jets by explicitly reconstructing the meson decay chain $D^{*+} \rightarrow D^0\pi^+ \rightarrow K^-\pi^+\pi^+$.

This paper discusses a complementary technique to measure the inclusive c -jet mistagging efficiency by means of a c -jet sample that is derived from $t\bar{t}$ events. The measurement uses a pp collision dataset which was collected with the ATLAS detector during 2015–2018 and corresponds to an integrated luminosity of 139 fb^{-1} . A likelihood-based method is used to select a high-purity $t\bar{t}$ sample in which one of the W bosons originating from the top-quark decay $t \rightarrow Wb$ decays leptonically into an electron or a muon plus the corresponding neutrino and the other decays hadronically. The branching ratio of a W boson to final states containing a charm-quark, which is approximately 33% [13], allows the c -jet mistagging efficiency of the data to be determined as a function of jet transverse momentum by fitting simulated event samples to the data sample. The technique has the advantage that it does not depend on a specific hadron decay chain topology.

* e-mail: atlas.publications@cern.ch

The measurement of the c -jet mistagging efficiency presented in this paper uses particle-flow (PFlow) jets, which are made by combining calorimeter energy deposits with inner-detector tracks [14], but the same technique is also used to make measurements for jets made only from calorimeter energy deposits [15] and jets that only use tracks (track-jets) [16].

This paper is structured as follows. Section 2 describes the ATLAS detector. Data and simulated samples are discussed in Sect. 3. The reconstruction of electrons, muons, jets and missing transverse momentum is described in Sect. 4, and the b -tagging algorithms are discussed in Sect. 5. The selection of the $t\bar{t}$ sample is described in Sect. 6. The measurement of the c -jet mistagging efficiency is described in Sect. 7, and Sect. 8 gives the conclusions.

2 ATLAS detector

The ATLAS detector [1] is a multipurpose particle physics detector with a forward–backward symmetric cylindrical geometry and nearly 4π coverage in solid angle.¹ The inner tracking detector consists of silicon pixel and microstrip detectors covering the pseudorapidity region $|\eta| < 2.5$, surrounded by a transition radiation tracker which enhances electron identification in the region $|\eta| < 2.0$. Between Run 1 and Run 2, a new inner pixel layer, the insertable B-layer [17, 18], was added at a mean sensor radius of 3.3 cm. The inner detector is surrounded by a thin superconducting solenoid providing an axial 2 T magnetic field, and by a fine-granularity lead/liquid-argon (LAr) electromagnetic calorimeter covering $|\eta| < 3.2$. A steel/scintillator-tile calorimeter provides hadronic coverage in the central pseudorapidity range ($|\eta| < 1.7$). The endcap and forward regions ($1.5 < |\eta| < 4.9$) of the hadronic calorimeter are made of LAr active layers with either copper or tungsten as the absorber material. An extensive muon spectrometer (MS) with an air-core toroidal magnet system surrounds the calorimeters. Three layers of high-precision tracking chambers provide coverage in the range $|\eta| < 2.7$, while dedicated fast chambers allow triggering in the region $|\eta| < 2.4$. The ATLAS trigger system consists of a hardware-based level-1

¹ ATLAS uses a right-handed coordinate system with its origin at the nominal interaction point in the centre of the detector. The positive x -axis is defined by the direction from the interaction point to the centre of the LHC ring, with the positive y -axis pointing upwards, while the beam direction defines the z -axis. Cylindrical coordinates (r, ϕ) are used in the transverse plane, ϕ being the azimuthal angle around the z -axis. The component of momentum in the transverse plane is denoted by p_T . The pseudorapidity η is defined in terms of the polar angle θ by $\eta = -\ln \tan(\theta/2)$. Rapidity is defined as $y = 0.5 \ln[(E + p_z)/(E - p_z)]$ where E denotes the energy, and p_z is the component of the momentum along the beam direction. The separation of two objects in η – ϕ space is given by $\Delta R = \sqrt{(\Delta\eta)^2 + (\Delta\phi)^2}$.

trigger followed by a software-based high-level trigger [19]. An extensive software suite [20] is used in the reconstruction and analysis of real and simulated data, in detector operations, and in the trigger and data acquisition systems of the experiment.

3 Data and simulated event samples

The data analysed in this paper correspond to 139 fb^{-1} [21, 22] of pp collision data collected by the ATLAS detector between 2015 and 2018 with a centre-of-mass energy of 13 TeV and a 25 ns proton bunch crossing interval. The data sample was collected using a set of single-electron [23] and single-muon [24] triggers with p_T thresholds in the range of 20–26 GeV depending on the lepton flavour and data-taking period. All detector subsystems were required to be operational during data taking and to fulfil data quality requirements. Events with noise bursts or coherent noise in the calorimeters are removed. The presence of additional interactions in the same bunch crossing, referred to as pile-up, is characterised by the average number of such interactions, $\langle\mu\rangle$, which was 34 for the whole dataset.

Simulated event samples are used to model SM processes and to estimate the expected signal yields. All samples were produced using the ATLAS simulation infrastructure [25] and GEANT4 [26]. A subset of samples used a faster simulation based on a parameterisation for the calorimeter response and GEANT4 for the other detector systems [25]. The simulated events are reconstructed with the same algorithms as used for data, and contain a realistic modelling of pile-up interactions. The pile-up profiles in the simulation match those of each dataset between 2015 and 2018, and were obtained by overlaying the hard-scatter events with minimum-bias events simulated using the soft QCD processes of PYTHIA 8 [27] with the NNPDF3.0LO set [28] of parton distribution functions (PDFs) [29] and a set of tuned parameters called the A3 tune [30]. For all samples, with the exception of those generated using SHERPA [31], the decays of bottom and charm hadrons were performed by EVTGEN [32].

The events used in this study originate mostly from $t\bar{t}$ production. This process was modelled using the POWHEG BOX v2 [33–36] generator at next-to-leading order (NLO) with the NNPDF3.0NLO PDF set [28] and the h_{damp} parameter² set to $1.5 \times m_{\text{top}}$ [37], where m_{top} denotes the mass of the top quark. The events were interfaced to PYTHIA 8.230 to model the parton shower, hadronisation, and underlying event, with

² The h_{damp} parameter is a resummation damping factor and one of the parameters that controls the matching of POWHEG matrix elements to the parton shower and thus effectively regulates the high- p_T radiation against which the $t\bar{t}$ system recoils.

parameters set according to the A14 tune [38] and using the NNPDF2.3LO set of PDFs [28]. The uncertainty due to initial-state radiation (ISR) is estimated by simultaneous variations of the h_{damp} parameter and the renormalisation and factorisation scales, and choosing the Var3c up/down variants of the A14 tune. The impact of final-state radiation (FSR) is evaluated by varying the renormalisation scale for emissions from the parton shower by a factor two up or down. The impact of using a different parton shower and hadronisation model is evaluated by comparing the nominal $t\bar{t}$ sample with another $t\bar{t}$ sample generated by POWHEG BOX v2 using exactly the same parameters but interfaced to HERWIG 7.04 [39,40], using the H7UE tune [40] and the MMHT2014LO PDF set [41].

In addition to $t\bar{t}$ production, some minor backgrounds contribute to the final event sample used for the calibration. These backgrounds consist mostly of single-top and diboson production, the production of $t\bar{t}$ in association with a vector boson and the production of a vector boson in association with jets. Details of the modelling of these samples are given in the following.

Single-top s -channel production was modelled using the POWHEG BOX v2 generator at NLO in QCD in the five-flavour scheme with the NNPDF3.0NLO PDF set. Single-top t -channel production was modelled using the POWHEG BOX v2 generator at NLO in QCD, using the four-flavour scheme and the corresponding NNPDF3.0NLO set of PDFs. The associated production of a single top quark and a W boson (tW) was modelled using the POWHEG BOX v2 generator at NLO in QCD, using the five-flavour scheme and the NNPDF3.0NLO set of PDFs. The diagram removal scheme [42] was used to remove interference and overlap with $t\bar{t}$ production. The events for all single-top production channels were interfaced to PYTHIA 8.230 using the A14 tune and the NNPDF2.3LO set of PDFs.

The production of Z +jets and W +jets events was simulated with the SHERPA 2.2.1 generator using NLO matrix elements for up to two partons, and leading-order (LO) matrix elements for up to four partons calculated with the Comix [43] and OPENLOOPS [44–46] libraries. They were matched with the SHERPA parton shower [47] using the MEPS@NLO prescription [48–51] and the set of tuned parameters developed by the SHERPA authors. The NNPDF3.0NNLO set of PDFs [28] was used and the samples were normalised to a next-to-next-to-leading-order (NNLO) prediction [52].

Samples of events with diboson final states (VV) were simulated with the SHERPA 2.2.1 or 2.2.2 generator depending on the process, including off-shell effects and Higgs boson contributions where appropriate. Fully leptonic final states and semileptonic final states, where one boson decays leptonically and the other hadronically, were generated using matrix elements at NLO accuracy in QCD for up to one addi-

tional parton and at LO accuracy for up to three additional parton emissions. Event samples for the loop-induced processes $gg \rightarrow VV$ were generated using LO-accurate matrix elements for up to one additional parton emission for both the fully leptonic and semileptonic final states. The matrix element calculations were matched and merged with the SHERPA parton shower based on Catani–Seymour dipole factorisation [43,47] using the MEPS@NLO prescription. The virtual QCD corrections were provided by the OPENLOOPS library. The NNPDF3.0NNLO set of PDFs was used, along with the dedicated set of tuned parton-shower parameters developed by the SHERPA authors.

Production of $t\bar{t}$ in association with a vector boson was modelled using the MADGRAPH5_aMC@NLO 2.3.3 [53] generator at NLO with the NNPDF3.0NLO PDF set. The events were interfaced to PYTHIA 8.210 [27] using the A14 tune and the NNPDF2.3LO PDF set.

4 Object reconstruction

Selected events are required to contain at least one vertex having at least two associated tracks with $p_T > 500$ MeV, and the primary vertex is chosen to be the vertex reconstructed with the largest Σp_T^2 of its associated tracks.

Electron candidates are reconstructed by matching inner-detector tracks to clusters of energy deposited in the EM calorimeter. Electrons must have $p_T > 27$ GeV and $|\eta| < 2.47$. The associated track must have $|d_0|/\sigma_{d_0} < 5$ and $|z_0| \sin \theta < 0.5$ mm, where d_0 (z_0) is the transverse (longitudinal) impact parameter relative to the primary vertex and σ_{d_0} is the uncertainty in d_0 . Candidates are identified with a likelihood method and must satisfy the ‘medium’ identification criteria described in Ref. [54]. The likelihood relies on the shape of the EM shower measured in the calorimeter, the quality of the track reconstruction, and the quality of the match between the track and the cluster. To suppress candidates originating from photon conversions, hadron decays, or jets misidentified as electrons, candidates are required to satisfy the gradient isolation criteria based on tracking and calorimeter measurements [54]. The electron energy and reconstruction efficiency are calibrated using $Z \rightarrow e^+e^-$ decays [54].

Muon candidates are reconstructed in the range $|\eta| < 2.5$ by combining tracks in the inner detector with tracks in the MS. All muon candidates must have $p_T > 27$ GeV, $|d_0|/\sigma_{d_0} < 3$, and $|z_0| \sin \theta < 0.5$ mm. The ‘medium’ quality requirements described in Ref. [55] are used and muons from hadron decays are suppressed by imposing a track-based isolation requirement. The muon reconstruction efficiency in the simulation is corrected using comparisons with data [56].

Jets are formed using objects from a particle-flow algorithm, which combines energy deposits in the calorimeter

with inner detector tracks [14]. The PFlow objects are combined into jets in the range $|\eta| < 2.5$ and $p_T > 20$ GeV using the anti- k_t algorithm [57, 58] with a radius parameter R of 0.4. A jet-vertex-tagging technique using a multivariate likelihood [59] is applied to jets with $|\eta| < 2.4$ and $p_T < 60$ GeV to suppress jets that are not associated with the event's primary vertex. Jets are further calibrated according to in situ measurements of the jet energy scale [15].

The labelling scheme used to define the flavour of a jet in a simulated event is applied by matching reconstructed jets to generator-level b - or c -hadrons with $p_T > 5$ GeV within a cone of size $\Delta R = 0.3$ around the jet axis. Jets that contain a b -hadron are called b -jets. Remaining jets containing a c -hadron are called c -jets. Jets with a hadronically decaying τ -lepton are called τ -jets, and all remaining jets are called light-flavour jets.

Overlaps between reconstructed objects are removed using a procedure based on the angular separation between different final-state objects. The procedure is similar to the one described in Ref. [60].

The event's missing transverse momentum, whose magnitude is denoted by E_T^{miss} , is computed as the negative vectorial sum of the transverse momenta of leptons, jets and a track-based soft term [61] accounting for the contribution from particles from the primary vertex that are not already included. The jets employed in the E_T^{miss} calculation include PFlow jets and, in addition, anti- k_t $R = 0.4$ jets with $p_T > 30$ GeV and $2.5 < |\eta| < 4.5$.

5 Description of b -tagging algorithms

Jets that contain a b -hadron are distinguished from other jets that contain a c -hadron or only light-flavour hadrons mainly by the larger mass and longer lifetime of the b -hadron. The b -tagging algorithm studied in this paper is called DL1r, and is an updated version of the DL1 tagger described in Ref. [62]. Information from the tracks in the jet, such as their transverse impact parameter and the reconstructed secondary and tertiary vertices, are combined into a set of low-level taggers. The DL1 algorithm combines the output of the low-level taggers into a single discriminant by using a deep neural network. DL1r adds the result of the RNNIP algorithm, which is based on a recurrent neural network exploiting the correlation between the tracks' impact parameters. Current analyses in ATLAS use the DL1r discriminant in intervals defined by the efficiency to tag b -jets in simulated $t\bar{t}$ events [10]. The b -tagging interval boundaries are 0, 60, 70, 77, 85 and 100%.

Measurements of the tagging efficiency SFs for b -jets are made as a function of jet p_T for $|\eta| < 2.5$, using $t\bar{t}$ events where both top quarks decay leptonically and a method similar to that described in Ref. [10]. The SFs for the mistagging efficiency for light-flavour jets are obtained by defining a

'flipped tagger' in which the sign of the track impact parameters that are used in the low-level taggers is inverted [11]. This results in similar efficiencies for light- and heavy-flavour jets, allowing the light-flavour SFs to be determined. Both the b - and light-flavour jet SFs have been determined using the full Run 2 dataset. It should be noted that both sets of SFs require a determination of the c -jet SFs, which were taken from a preliminary version of the method described in this paper. Since the contamination from c -jets is relatively small in these measurements and because the previous SFs were similar to those in the present measurement, any differences only have a small impact.

Analyses that use b -tagging in ATLAS apply a weight to each simulated event, derived as the product of the SFs for all jets for which a tagging requirement is made. It is found that there are significant differences between the simulated (mis)tagging efficiency for different fragmentation models [10]. To account for these differences, simulation-to-simulation SFs are applied to those simulated samples that have a fragmentation model and decay different from the one used to derive the SFs. In the present paper the $t\bar{t}$ simulation (see Sect. 3) uses PYTHIA 8 and EVTGEN, which is the reference MC fragmentation program for all the measured SFs.

6 Event selection and reconstruction

The analysis aims to obtain a pure sample of semileptonic $t\bar{t}$ events. Exactly one electron or one muon, denoted by ℓ , is required. The events are also required to have $E_T^{\text{miss}} > 20$ GeV, and the transverse mass m_T of the E_T^{miss} and the lepton must satisfy

$$m_T = \sqrt{2p_T^\ell E_T^{\text{miss}}(1 - \cos \Delta\phi)} > 40 \text{ GeV},$$

where $\Delta\phi = \phi(E_T^{\text{miss}}) - \phi(\ell)$ is the azimuthal angle between the lepton and E_T^{miss} . Subsequently, a requirement on the number of PFlow jets is applied such that one of the following selections is true:

- the event contains exactly four jets with $p_T > 25$ GeV
- the event contains at least three jets with $p_T > 25$ GeV and exactly one jet with $20 < p_T < 25$ GeV
- the event contains at least five jets with $p_T > 25$ GeV and at least one of these jets has $p_T > 70$ GeV.

These selections are designed to keep a high number of jets covering a large range in p_T , while reducing the non- $t\bar{t}$ background and the number of jets arising from final state QCD radiation (FSR). The first requirement is the 'baseline' selection, which has a relatively low rate of FSR jets, due to requiring exactly four jets. The second requirement allows measurements to be made for jets between $20 < p_T < 25$ GeV,

while minimising the non- $t\bar{t}$ background which is more likely to have multiple low p_T jets. The third requirement improves the statistics of high p_T jets where the rate of FSR is greater. Although allowing five jets increases the fraction FSR jets being included in the selection, the rate of such jets is reasonable for jet $p_T > 70$ GeV, since the likelihood, described below, is better able to identify the top decay products at higher p_T .

The four-vectors of the four highest- p_T jets, the lepton and the event E_T^{miss} are used as inputs to a likelihood-based $t\bar{t}$ event reconstruction algorithm, which minimises deviations in the invariant masses of the top quarks and W bosons from their true values and is described in more detail in Ref. [63]. This algorithm uses a likelihood function to assign the four jets to the $t\bar{t}$ decay topology. In particular, the algorithm assigns one jet to the b -jet from the leptonically decaying top quark ($t \rightarrow Wb \rightarrow \ell\nu b$), another jet to the b -jet from the hadronically decaying top quark ($t \rightarrow Wb \rightarrow qq'b$, where qq' are the quarks into which the W boson decays) and the remaining two jets to the jets that come from the hadronic W boson decay. The jet assignment does not use any b -tagging information. The following notation is used: the jets that are assigned as the decay products of the W boson are referred to as W -jets and the remaining two jets are referred to as top-jets.

The four-jet combination that has the highest likelihood is selected for the $t\bar{t}$ reconstruction only if the negative logarithm of the likelihood value is greater than -48 . This requirement increases the fraction of events where the top-quark decay products are correctly assigned. Subsequently, the top-jets are required to lie in the tightest (0–60%) DL1r b -tagging interval, whereas no b -tagging requirement is imposed on the W -jets, so as to leave them unbiased. After these requirements it is found that 98.8% of events in the $t\bar{t}$ simulation have two top-jets that are b -jets.

The distribution of the value of the negative logarithm of the likelihood for the selected events is shown in Fig. 1. The majority of the events come from $t\bar{t}$ production with 3% of the events, referred to as ‘non $t\bar{t}$ ’, coming from other processes such as W +jets or Z +jets production or single-top production. The simulated $t\bar{t}$ events are categorised according to the flavour of the W -jets. The notation ‘ ll ’ indicates that both W -jets are light-flavour jets. Similarly, ‘ cl ’ (‘ bl ’) indicates that one of the W -jets is a c -jet (b -jet) and the other is a light-flavour jet. The W -jet pairs with flavours other than those discussed above fall into a category called ‘other’, which also includes events in which at least one of the W -jets comes from a hadronically decaying τ -lepton. The ll category accounts for 55% of events, the cl category for 41%, the bl category for 1.8% and the ‘other’ category for 2.5%.

The simulated $t\bar{t}$ yield shown in Fig. 1, as well as in all subsequent figures and results in this paper, is corrected for compatibility with ATLAS $t\bar{t}$ measurements [64], which

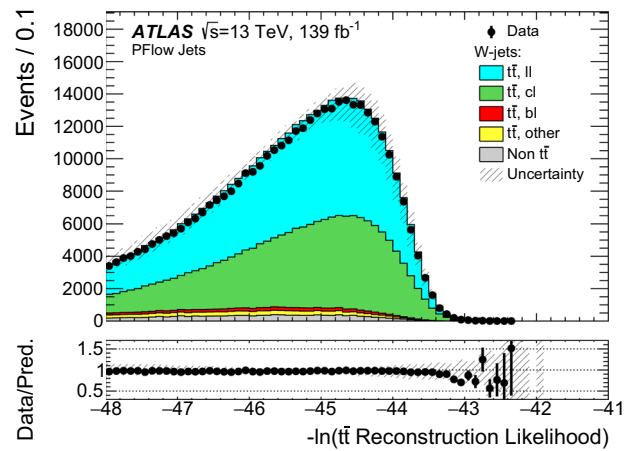


Fig. 1 Distribution of the negative logarithm of the likelihood that is used to reconstruct the $t\bar{t}$ decay. Only events with values of this quantity exceeding -48 are shown, which corresponds to the selection used in the measurement. The $t\bar{t}$ simulation is split according to the flavours of the W -jets (ll , cl , bl and other). The (mis)tagging efficiency scale factors have not been applied to the simulation. The hashed area shows the total uncertainty, excluding the uncertainties from the (mis)tagging efficiency scale factors and the uncertainty on the jet p_T distribution, which is derived from the difference between data and simulation

indicate that the simulation underestimates the number of events containing more than two b -jets. For this reason, simulated events in which both the top-jets and at least one of the W -jets are b -jets are scaled by 1.25 ± 0.25 , where the full difference between data and the prediction from simulation is taken as a systematic uncertainty. The remaining events are normalised using the prediction from simulation. Finally, Fig. 1 includes an uncertainty in the simulation estimate (see Sect. 7.2), derived as the combination of the detector systematic uncertainties, the $t\bar{t}$ modelling uncertainties and the uncertainty due to the limited number of simulated events.

The η and p_T distributions of the W -jets that are selected with the procedure described above are shown in Fig. 2. Although the simulation generally describes the data well, it can be seen that it has a slightly harder p_T spectrum than the data. This difference is included as a systematic error as described in Sect. 7.2. Figure 2 also shows the DL1r discriminant, where it can be seen that the simulation describes the data reasonably well, but there are some differences, particularly at high and low DL1r discriminant values.

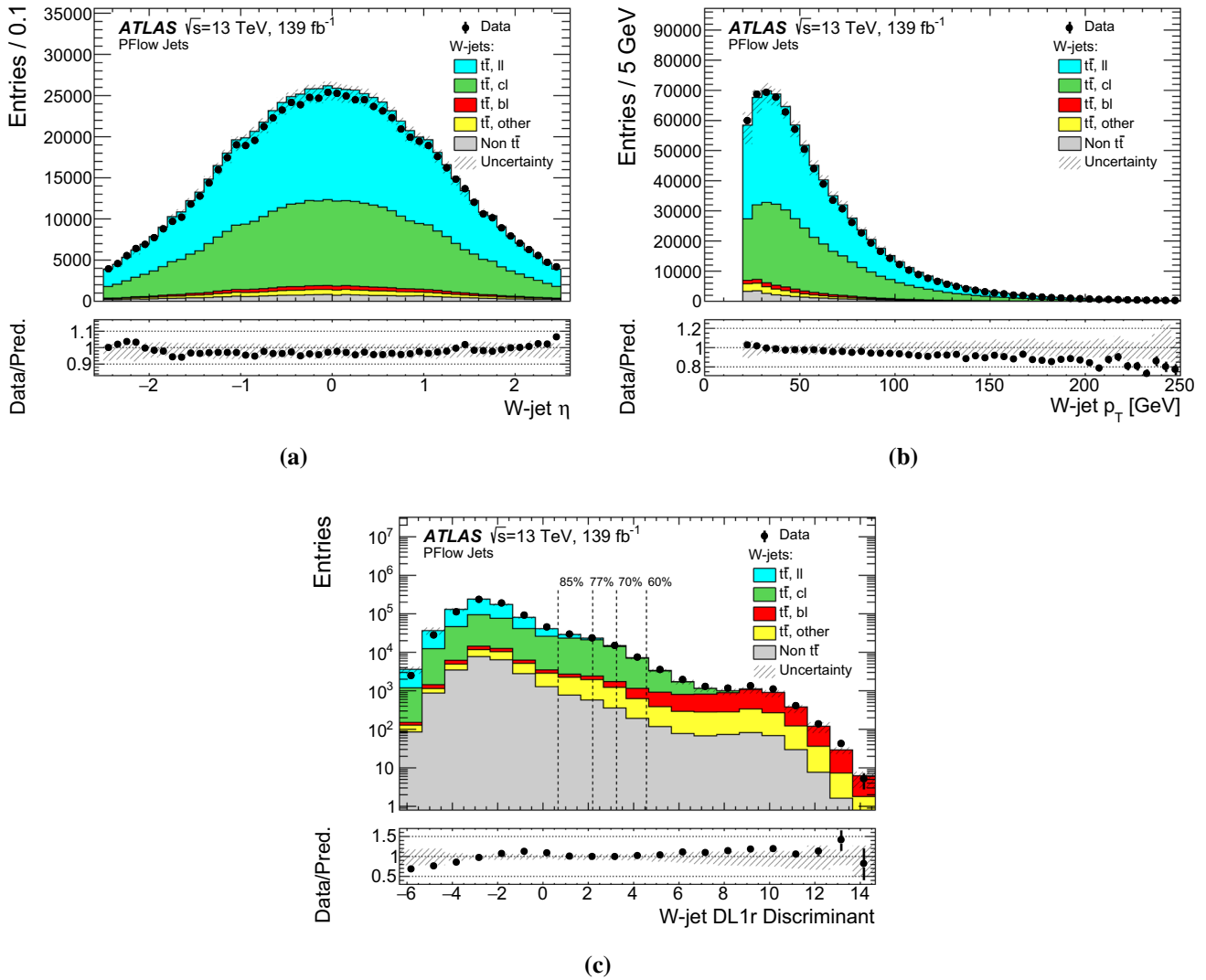


Fig. 2 Distributions of **a** η , **b** p_T and **c** the DL1r discriminant for the particle-flow jets that are associated with the W boson decay by the likelihood-based $t\bar{t}$ event reconstruction algorithm (W -jets). The $t\bar{t}$ simulation is split according to the flavours of the W -jets (ll , cl , bl and other). The (mis)tagging efficiency scale factors have not been applied

to the simulation. The hashed area shows the total uncertainty, excluding the uncertainties from the (mis)tagging efficiency scale factors and the uncertainty on the jet p_T distribution, which is derived from the difference between data and simulation. The vertical dashed lines in **c** indicate the DL1r discriminant tagging intervals

7 Measurement of the charm mistagging efficiency

7.1 Method

The c -jet mistagging efficiency is determined by comparing the fraction of events where either of the W -jets are tagged in data with the fraction tagged in simulation. The efficiency is evaluated in four jet- p_T intervals, with boundaries at 20, 40, 65, 140 and 250 GeV, and for the tagging intervals as described in Sect. 5. Jets are said to be tagged (untagged) if they have DL1r discriminant values greater (less) than the value at the 85% boundary. The method described below is for the ‘pseudo-continuous’ calibration where the efficiency

is defined as the fraction of c -jets that have a DL1r discriminant value that lies between the boundaries, i.e. a value greater than the 60% boundary, a value between the 70% and 60% boundaries, etc.

The light-flavour jet and b -jet SFs are taken from other measurements as described in Sect. 5 and the corresponding SFs are applied to the two W -jets and the two top-jets if they are light-flavour jets or b -jets. The remaining difference between the numbers of tagged W -jets events in data and simulation is used to determine the ratio of the c -jet mistagging efficiencies in data and simulation.

To simplify the fit, events where both W -jets are tagged, making up 0.7% of the total number of events, are rejected.

Table 1 The measured c -jet pseudo-continuous mistagging efficiency scale factors listed with the total, statistical and systematic uncertainties for particle-flow jets shown for each tagging and jet- p_T interval. The scale factors are listed for the PYTHIA 8+EVTGEN fragmentation model

Tagging interval (%)	Jet p_T range (GeV)	SF	Tot. (%)	Stat. (%)	Sys. (%)
85–100	20–40	1.014	6.0	1.6	5.8
85–100	40–65	1.013	2.9	1.6	2.4
85–100	65–140	0.999	2.6	1.6	2.1
85–100	140–250	1.014	3.0	2.1	2.2
77–85	20–40	0.963	12	1.7	12
77–85	40–65	0.960	4.8	1.1	4.7
77–85	65–140	0.967	4.1	1.1	4.0
77–85	140–250	0.968	5.4	2.9	4.6
70–77	20–40	0.907	10	1.6	10
70–77	40–65	0.965	5.1	1.4	4.9
70–77	65–140	0.996	4.0	1.4	3.8
70–77	140–250	0.964	5.0	3.7	3.4
60–70	20–40	1.028	11	2.0	11
60–70	40–65	0.972	5.1	1.8	4.8
60–70	65–140	1.038	4.9	2.0	4.5
60–70	140–250	1.040	6.0	5.1	3.1
0–60	20–40	1.173	17	3.9	17
0–60	40–65	1.180	13	3.5	12
0–60	65–140	1.214	10	3.8	9.2
0–60	140–250	0.934	15	9.0	12

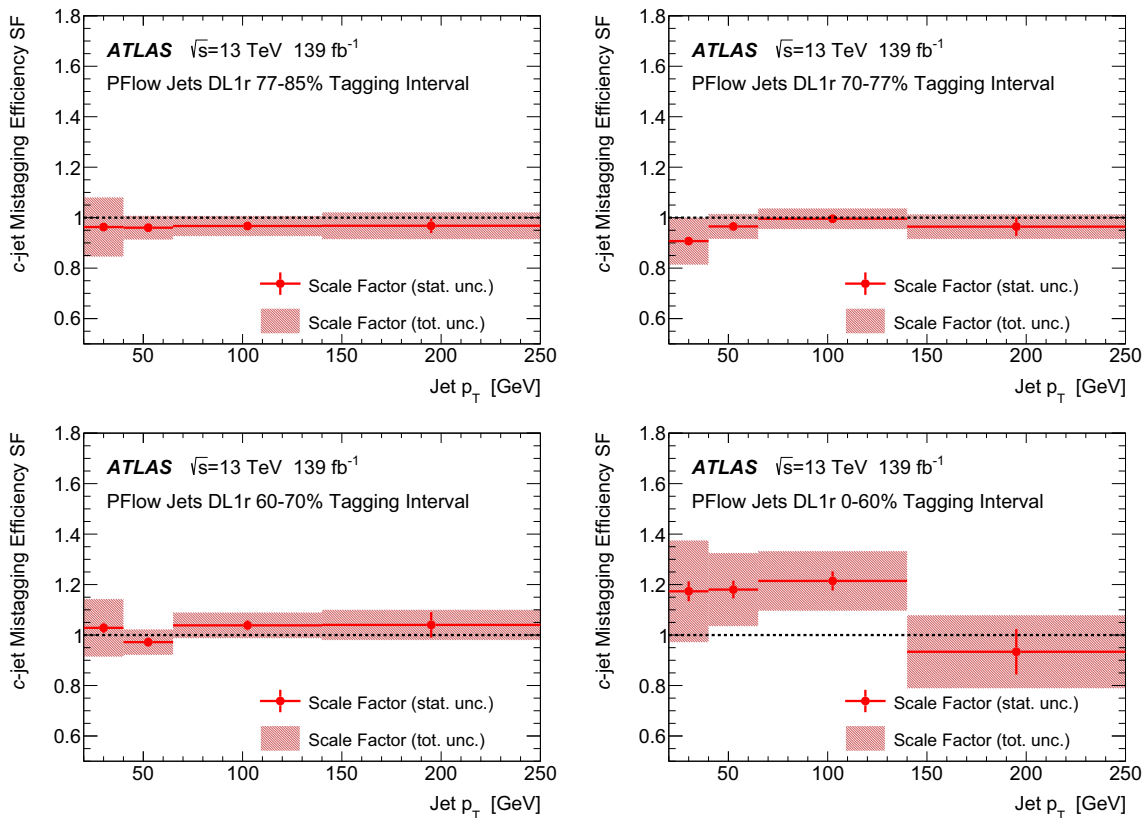


Fig. 3 The c -jet pseudo-continuous mistagging efficiency scale factors for particle-flow jets shown as a function of jet p_T for four tagging intervals. The scale factors are shown for the PYTHIA 8+EVTGEN fragmentation model

Table 2 The contributions to the c -jet pseudo-continuous mistagging efficiency scale factor systematic uncertainties for particle-flow jets. Listed are the uncertainties related to the $t\bar{t}$ modelling, the jets and E_T^{miss} , the light-flavour jet scale factor, the b -jet scale factor, and all other sources

Tagging interval (%)	Jet p_T range (GeV)	Systematic uncertainty in SF				
		$t\bar{t}$ mod. (%)	Jet/ E_T^{miss} (%)	Light tag (%)	b -tag (%)	Other (%)
85–100	20–40	5.3	0.8	2.3	–	0.1
85–100	40–65	2.1	0.3	1.2	–	–
85–100	65–140	1.9	0.2	0.9	–	0.1
85–100	140–250	2.0	0.4	0.9	–	0.1
77–85	20–40	8.3	3.1	8.2	–	0.3
77–85	40–65	3.0	1.0	3.5	–	0.1
77–85	65–140	3.2	0.5	2.4	–	0.2
77–85	140–250	3.9	0.9	2.3	–	0.3
70–77	20–40	9.7	1.2	2.5	–	0.4
70–77	40–65	4.7	0.8	1.1	–	0.1
70–77	5–140	3.7	0.4	0.8	–	0.2
70–77	140–250	3.1	1.0	0.9	–	0.1
60–70	20–40	11	0.8	1.6	–	0.4
60–70	40–65	4.7	0.6	0.9	–	0.1
60–70	65–140	4.4	0.4	0.6	–	0.2
60–70	140–250	2.6	1.4	0.8	0.2	0.2
0–60	20–40	17	3.1	0.8	0.2	1.5
0–60	40–65	11	3.7	0.4	0.1	0.9
0–60	65–140	8.7	3.0	0.2	–	0.7
0–60	140–250	9.7	7.1	0.7	–	1.7

Events where both W -jets are untagged are retained to provide a normalisation of the simulation as described below. The data are divided into bins according to the tagging interval (labelled t , running from 1 to 4) and the p_T bin of the tagged W -jet (labelled i), and the p_T bin of the untagged W -jet (labelled j). The number of events in each bin is denoted by $N_{\text{data}}^t(i, j)$. In addition, the number of untagged data events is recorded in each W -jet p_T bin combination: $N_{\text{data}}^{\text{untag}}(i, j)$ where in this case the higher- p_T jet is denoted by j , so $j \geq i$.

The fit is performed by comparing data with the total expectation, which is dominated by $t\bar{t}$ events. The number of simulated ‘signal’ events in each bin, $N_C^t(i, j)$, is made up of those events where the tagged W -jet is a c -jet; the other jets in the event may be of any flavour. There are two sources of ‘background’ events, defined as events where the tagged W -jet is not a c -jet. The first is the number of events where neither of the top-jets is a c -jet, $N_J^t(i, j)$. The second arises from events where a c -jet is misclassified as one of the top-jets. This background requires a specific treatment since the c -jet is in a p_T bin, labelled k , different from those of the W -jets and so must be binned in this variable in addition to i and j . The number of events from this background is denoted by $N_X^t(i, j, k)$. The number of untagged simulated events is recorded in a similar way to the data as $N_{\text{MC}}^{\text{untag}}(i, j)$.

The free parameters in the fit are the c -jet mistagging SF in each p_T bin and tagging interval, $c^t(i)$, and the overall MC normalisation in each W -jet p_T combination, $p(i, j)$.

A fit is performed by minimising the χ^2 defined as:

$$\chi^2 = \sum_{t=1}^4 \sum_{i=1}^4 \sum_{j=1}^4 \left[N_{\text{data}}^t(i, j) - p(i, j) \left(c^t(i) N_C^t(i, j) + N_J^t(i, j) + \sum_{k=1}^4 c^{t=4}(k) N_X^t(i, j, k) \right) \right]^2 / N_{\text{data}}^t(i, j) + \sum_{i=1}^4 \sum_{j=i}^4 \left(N_{\text{data}}^{\text{untag}}(i, j) - p(i, j) N_{\text{MC}}^{\text{untag}}(i, j) \right)^2 / N_{\text{data}}^{\text{untag}}(i, j). \tag{1}$$

The background where one of the top-jets is a c -jet depends only on $c^{t=4}(k)$ since the top-jets are tagged at the 60% operating point. The SFs for c -jets that are untagged in each jet p_T bin, $c^{\text{untag}}(i)$, are evaluated by constraining the sum of the measured efficiencies of all tagged bins and the untagged bin to be 1. Technically, this is evaluated by adding additional terms to the χ^2 and treating the SFs $c^{\text{untag}}(i)$ as

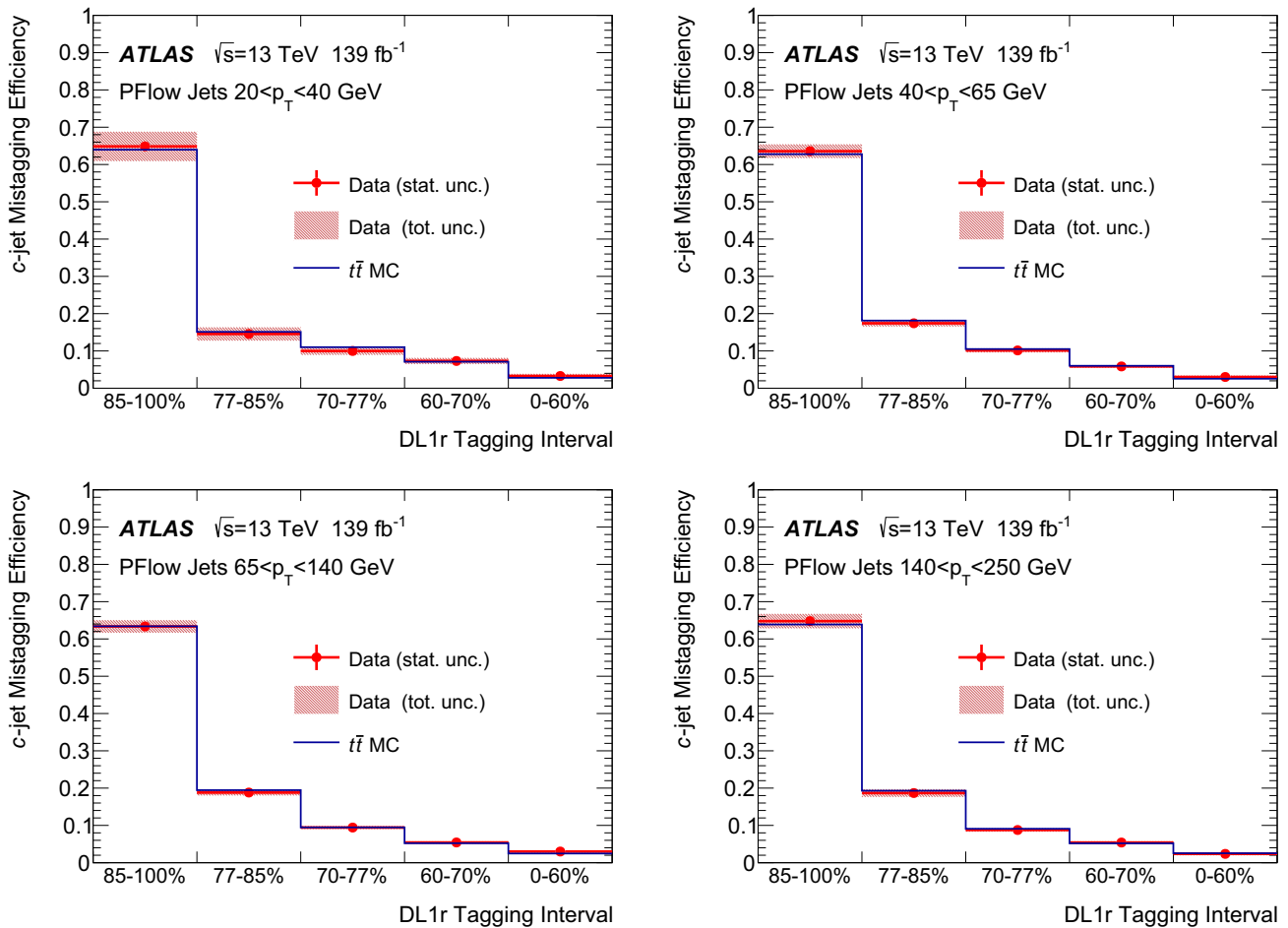


Fig. 4 The *c*-jet pseudo-continuous mistagging efficiencies for particle-flow jets shown as red points as a function of tagging interval for the four jet- p_T ranges. Included in the plots are the corresponding MC efficiencies using the PYTHIA 8+EVTGEN fragmentation model

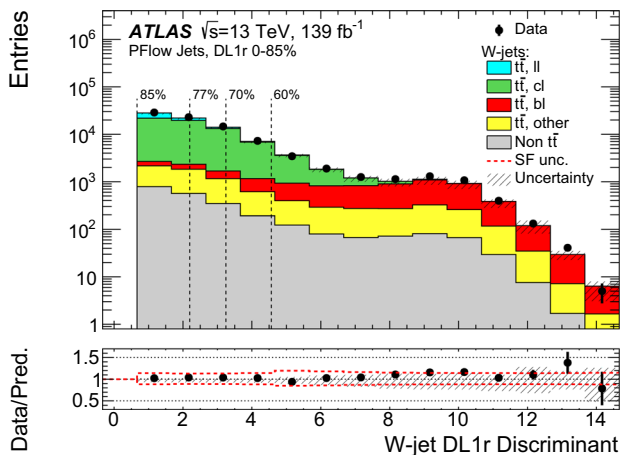


Fig. 5 The DL1r discriminant distribution for tagged particle-flow jets associated with the *W* boson decay (*W*-jets) after applying the *b*-, *c*- and light-flavour jet tagging scale factors to the simulation. The red dashed lines (bottom) show the uncertainty from the jet tagging scale factors, while the hashed area shows all other uncertainties excluding the uncertainty on the jet p_T distribution, which is derived from the difference between data and simulation. The vertical dashed lines indicate the DL1r discriminant tagging intervals

additional free parameters with an arbitrary tolerance of 1%:

$$\sum_{i=1}^4 \left(1 - c^{\text{untag}}(i) \epsilon_{\text{MC}}^{\text{untag}}(i) - \sum_{t=1}^4 c^t(i) \epsilon_{\text{MC}}^t(i) \right)^2 / (1\%)^2, \tag{2}$$

where $\epsilon_{\text{MC}}^{\text{untag}}(i)$ and $\epsilon_{\text{MC}}^t(i)$ are the MC untagged and tagged efficiencies, respectively. As part of validating the method it was checked that scale factors of unity are obtained when performing a fit with data replaced by the MC simulation.

7.2 Systematic uncertainties

Several sources of experimental and MC modelling systematic uncertainties affecting the *c*-jet efficiency SFs are considered. The uncertainty from each source is evaluated by making the corresponding change to the MC model and rederiving the SFs for each tagging interval and jet p_T bin. The total

systematic uncertainty for each bin is evaluated by adding the individual contributions in quadrature.

The uncertainties in the jet energy scale and resolution are based on their measurements in data [15] and result in shifts of up to 5% in the measured SFs due to a single component. Uncertainties in the track-based soft term of the E_T^{miss} [65] result in shifts of up to 3%. The uncertainty due to the pile-up modelling [66] leads to shifts of up to 0.7%. Uncertainties originating from the electron [54] and muon [56] reconstruction lead to shifts up to 0.5%. An additional uncertainty is applied to cover the W -jet p_T spectrum differences between data and simulation, giving a maximum uncertainty in the measured SFs of 0.2%.

The uncertainties in the light-flavour mistagging and b -jet tagging SFs are accounted for by shifting the SFs by each component of the total uncertainty, and where appropriate correlating this with the uncertainty used in the charm SF determination. The most important non-correlated uncertainties all come from the light-flavour SF. They originate from using the flipped tagger rather than standard tagger, giving

uncertainties of up to 7%, and from varying the charm SFs in the light-flavour SF determination, giving uncertainties of up to 4% [11].

Uncertainties in the modelling of the $t\bar{t}$ background are estimated by replacing the nominal MC sample by alternative MC samples. The uncertainty due to the choice of parton shower and hadronisation model is estimated by replacing the standard PYTHIA 8 model with HERWIG. This is the largest source of uncertainty in the analysis and leads to shifts of up to 13% in the SF. The uncertainty in the modelling of initial- and final-state radiation is assessed by increasing the radiation by doubling the h_{damp} parameter [37] and halving the renormalisation and factorisation scales and decreasing the radiation by increasing the scales by a factor of two. The resulting uncertainty is at most 1%. As already mentioned, the uncertainty in the normalisation of the $t\bar{t}+b\bar{b}$ process [64] is estimated by scaling the events where both the top-jets and at least one of the W -jets are b -jets by $\pm 25\%$, giving an uncertainty of up to 9% on the SF. The uncertainty in non-

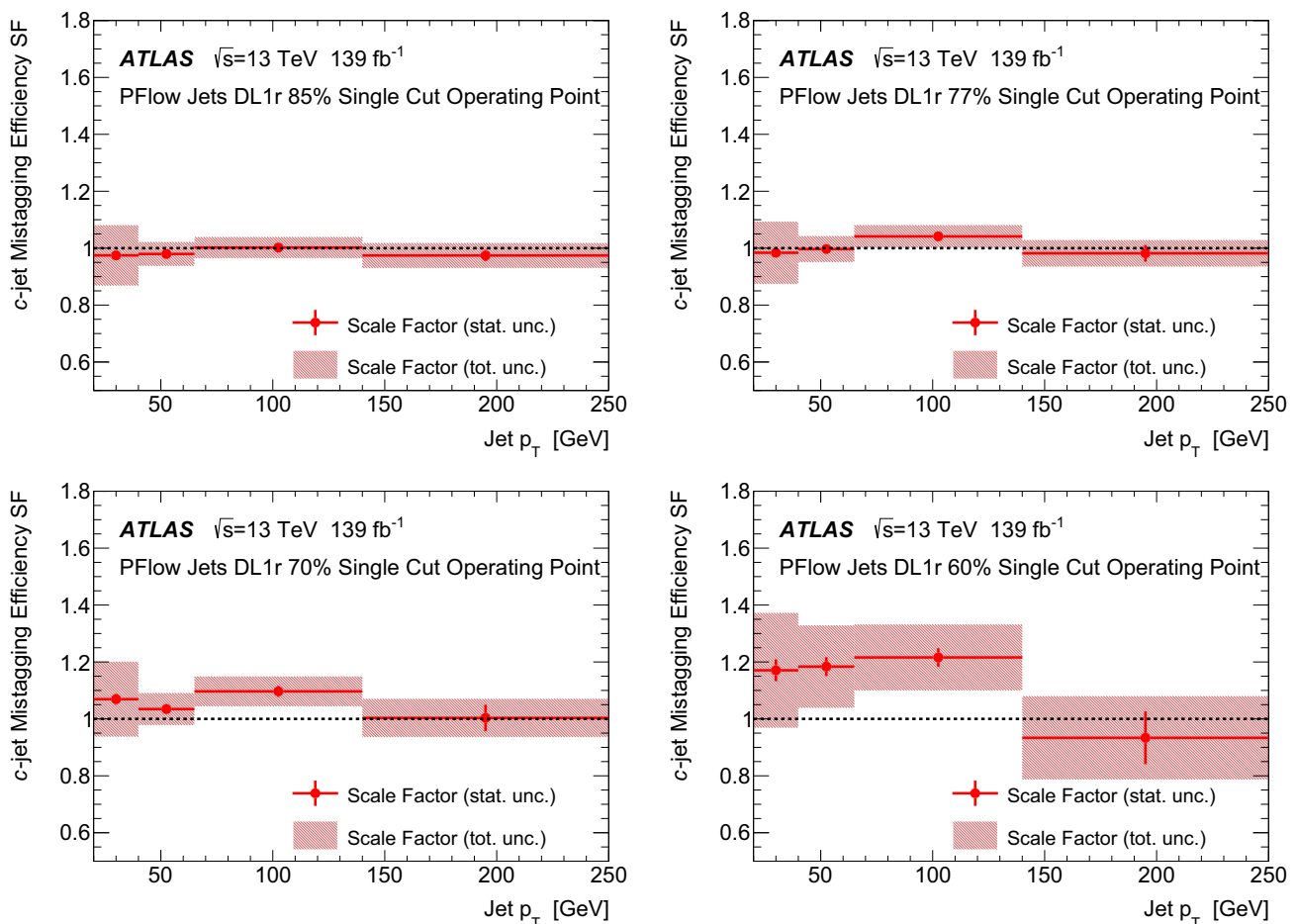


Fig. 6 The c -jet single-cut mistagging efficiency scale factors for particle-flow jets shown as a function of jet p_T for the four tagging operating points. The scale factors are shown for the PYTHIA 8+EVTGEN fragmentation model

$t\bar{t}$ processes is evaluated by scaling these contributions by $\pm 25\%$, leading to a maximum uncertainty of 1% on the SF.

7.3 Results

The measured c -jet pseudo-continuous mistagging efficiency SFs together with the total, statistical and systematic uncertainties are listed in Table 1 and shown in Fig. 3 for four tagging intervals. The fitted normalisation factors $p(i, j)$ lie in the range 0.83 to 1.05. The contributions to the systematic uncertainty are listed in Table 2. The corresponding measured data mistagging efficiencies, shown in Fig. 4, are obtained by multiplying the mistagging efficiencies from simulation by the SFs. The SFs do not have a strong jet- p_T dependence and are consistent with unity for all but the tightest tagging interval, where the efficiency is higher in data than in MC simulation. The total uncertainty varies from 3 to 17% and is dominated by the systematic uncertainty except in the highest p_T bin.

Figure 5 shows the DL1r discriminant distributions for tagged W -jets, after applying to simulation the light-flavour mistagging and b -tagging efficiency SFs, taken from other measurements as described in Sect. 5, and the c -jet SFs obtained from this analysis. It can be seen that the simulation agrees with the data within uncertainties over the entire distribution.

Many ATLAS analyses also use the SFs in a simplified form called ‘single cut’, where events are classified as tagged (untagged) if the DL1r discriminant lies above (below) one of the operating point boundaries. The corresponding SFs are determined in a similar way to the c -jet pseudo-continuous mistagging efficiency SFs by using Eq. (1), but replacing N_{data}^t , N_C^t , N_J^t and N_X^t with the corresponding numbers of events in which the tagged jet has a DL1r discriminant value above the operating point. The extra terms in Eq. (2) are not used in these fits. Instead the untagged SFs are evaluated using the results of the fit as $(1 - c^t(i)\epsilon_{\text{MC}}^t(i))/(1 - \epsilon_{\text{MC}}^t(i))$. The resulting single-cut c -jet mistagging efficiency SFs are shown in Fig. 6.

8 Conclusion

A new technique has been used to measure the inclusive c -jet mistagging efficiency, using semileptonic $t\bar{t}$ events from pp collisions at $\sqrt{s} = 13$ TeV at the LHC. The measurement is based on an integrated luminosity of 139 fb^{-1} , corresponding to the full Run 2 dataset, collected with the ATLAS detector. The efficiencies were measured as a function of jet p_T in the range 20–250 GeV, with boundaries correspond-

ing to 60, 70, 77 and 85% efficiency to tag b -jets in simulated $t\bar{t}$ events. The total uncertainties are in the range 3–17%. The measured efficiencies generally agree with those in simulation but are higher for the tightest (0–60%) tagging interval.

Acknowledgements We thank CERN for the very successful operation of the LHC, as well as the support staff from our institutions without whom ATLAS could not be operated efficiently. We acknowledge the support of ANPCyT, Argentina; YerPhI, Armenia; ARC, Australia; BMWFW and FWF, Austria; ANAS, Azerbaijan; SSTC, Belarus; CNPq and FAPESP, Brazil; NSERC, NRC and CFI, Canada; CERN; ANID, Chile; CAS, MOST and NSFC, China; Minciencias, Colombia; MSMT CR, MPO CR and VSC CR, Czech Republic; DNRF and DNSRC, Denmark; IN2P3-CNRS and CEA-DRF/IRFU, France; SRNSFG, Georgia; BMBF, HGF and MPG, Germany; GSRI, Greece; RGC and Hong Kong SAR, China; ISF and Benozio Center, Israel; INFN, Italy; MEXT and JSPS, Japan; CNRST, Morocco; NWO, Netherlands; RCN, Norway; MNiSW and NCN, Poland; FCT, Portugal; MNE/IFA, Romania; JINR; MES of Russia and NRC KI, Russian Federation; MESTD, Serbia; MSSR, Slovakia; ARRS and MIZŠ, Slovenia; DSI/NRF, South Africa; MICINN, Spain; SRC and Wallenberg Foundation, Sweden; SERI, SNSF and Cantons of Bern and Geneva, Switzerland; MOST, Taiwan; TAEK, Turkey; STFC, United Kingdom; DOE and NSF, United States of America. In addition, individual groups and members have received support from BCKDF, CANARIE, Compute Canada and CRC, Canada; COST, ERC, ERDF, Horizon 2020 and Marie Skłodowska-Curie Actions, European Union; Investissements d’Avenir Labex, Investissements d’Avenir Idex and ANR, France; DFG and AvH Foundation, Germany; Herakleitos, Thales and Aristeia programmes co-financed by EU-ESF and the Greek NSRF, Greece; BSF-NSF and GIF, Israel; Norwegian Financial Mechanism 2014–2021, Norway; La Caixa Banking Foundation, CERCA Programme Generalitat de Catalunya and PROMETEO and GenT Programmes Generalitat Valenciana, Spain; Göran Gustafssons Stiftelse, Sweden; The Royal Society and Leverhulme Trust, United Kingdom. The crucial computing support from all WLCG partners is acknowledged gratefully, in particular from CERN, the ATLAS Tier-1 facilities at TRIUMF (Canada), NDGF (Denmark, Norway, Sweden), CC-IN2P3 (France), KIT/GridKA (Germany), INFN-CNAF (Italy), NL-T1 (Netherlands), PIC (Spain), ASGC (Taiwan), RAL (UK) and BNL (USA), the Tier-2 facilities worldwide and large non-WLCG resource providers. Major contributors of computing resources are listed in Ref. [67].

Data Availability Statement This manuscript has no associated data or the data will not be deposited. [Authors’ comment: “All ATLAS scientific output is published in journals, and preliminary results are made available in Conference Notes. All are openly available, without restriction on use by external parties beyond copyright law and the standard conditions agreed by CERN. Data associated with journal publications are also made available: tables and data from plots (e.g. cross section values, likelihood profiles, selection efficiencies, cross section limits,...) are stored in appropriate repositories such as HEPDATA (<http://hepdata.cedar.ac.uk/>). ATLAS also strives to make additional material related to the paper available that allows a reinterpretation of the data in the context of new theoretical models. For example, an extended encapsulation of the analysis is often provided for measurements in the framework of RIVET (<http://rivet.hepforge.org/>).” This information is taken from the ATLAS Data Access Policy, which is a public document that can be downloaded from <http://opendata.cern.ch/record/413> [opendata.cern.ch].]

Open Access This article is licensed under a Creative Commons Attribution 4.0 International License, which permits use, sharing, adaptation,

distribution and reproduction in any medium or format, as long as you give appropriate credit to the original author(s) and the source, provide a link to the Creative Commons licence, and indicate if changes were made. The images or other third party material in this article are included in the article's Creative Commons licence, unless indicated otherwise in a credit line to the material. If material is not included in the article's Creative Commons licence and your intended use is not permitted by statutory regulation or exceeds the permitted use, you will need to obtain permission directly from the copyright holder. To view a copy of this licence, visit <http://creativecommons.org/licenses/by/4.0/>.
Funded by SCOAP³.

References

- ATLAS Collaboration, The ATLAS experiment at the CERN large hadron collider. *JINST* **3**, S08003 (2008). <https://doi.org/10.1088/1748-0221/3/08/S08003>
- L. Evans, P. Bryant, LHC machine. *JINST* **3**, S08001 (2008). <https://doi.org/10.1088/1748-0221/3/08/S08001>
- ATLAS Collaboration, Observation of the associated production of a top quark and a Z boson in pp collisions at $\sqrt{s} = 13$ TeV with the ATLAS detector. *JHEP* **07**, 124 (2020). [https://doi.org/10.1007/JHEP07\(2020\)124](https://doi.org/10.1007/JHEP07(2020)124). [arXiv:2002.07546](https://arxiv.org/abs/2002.07546) [hep-ex]
- ATLAS Collaboration, Measurements of the production cross-section for a Z boson in association with b -jets in proton–proton collisions at $\sqrt{s} = 13$ TeV with the ATLAS detector. *JHEP* **07**, 044 (2020). [https://doi.org/10.1007/JHEP07\(2020\)044](https://doi.org/10.1007/JHEP07(2020)044). [arXiv:2003.11960](https://arxiv.org/abs/2003.11960) [hep-ex]
- ATLAS Collaboration, Observation of $H \rightarrow b\bar{b}$ decays and VH production with the ATLAS detector. *Phys. Lett. B* **786**, 59 (2018). <https://doi.org/10.1016/j.physletb.2018.09.013>. [arXiv:1808.08238](https://arxiv.org/abs/1808.08238) [hep-ex]
- ATLAS Collaboration, Observation of Higgs boson production in association with a top quark pair at the LHC with the ATLAS detector. *Phys. Lett. B* **784**, 173 (2018). <https://doi.org/10.1016/j.physletb.2018.07.035>. [arXiv:1806.00425](https://arxiv.org/abs/1806.00425) [hep-ex]
- ATLAS Collaboration, Search for pairs of scalar leptoquarks decaying into quarks and electrons or muons in $\sqrt{s} = 13$ TeV pp collisions with the ATLAS detector. *JHEP* **10**, 112 (2020). [https://doi.org/10.1007/JHEP10\(2020\)112](https://doi.org/10.1007/JHEP10(2020)112). [arXiv:2006.05872](https://arxiv.org/abs/2006.05872) [hep-ex]
- ATLAS Collaboration, Search for phenomena beyond the Standard Model in events with large b -jet multiplicity using the ATLAS detector at the LHC. *Eur. Phys. J. C* **81**, 11 (2021). <https://doi.org/10.1140/epjc/s10052-020-08730-0>. [arXiv:2010.01015](https://arxiv.org/abs/2010.01015) [hep-ex]
- ATLAS Collaboration, Measurements of b -jet tagging efficiency with the ATLAS detector using $t\bar{t}$ events at $\sqrt{s} = 13$ TeV. *JHEP* **08**, 089 (2018). [https://doi.org/10.1007/JHEP08\(2018\)089](https://doi.org/10.1007/JHEP08(2018)089). [arXiv:1805.01845](https://arxiv.org/abs/1805.01845) [hep-ex]
- ATLAS Collaboration, ATLAS b -jet identification performance and efficiency measurement with $t\bar{t}$ events in pp collisions at $\sqrt{s} = 13$ TeV. *Eur. Phys. J. C* **79**, 970 (2019). <https://doi.org/10.1140/epjc/s10052-019-7450-8>. [arXiv:1907.05120](https://arxiv.org/abs/1907.05120) [hep-ex]
- ATLAS Collaboration, Calibration of light-flavour b -jet mistagging rates using ATLAS proton–proton collision data at $\sqrt{s} = 13$ TeV. ATLAS-CONF-2018-006 (2018). <https://cds.cern.ch/record/2314418>
- ATLAS Collaboration, Performance of b -jet identification in the ATLAS experiment. *JINST* **11**, P04008 (2016). <https://doi.org/10.1088/1748-0221/11/04/P04008>. [arXiv:1512.01094](https://arxiv.org/abs/1512.01094) [hep-ex]
- P.A. Zyla et al., Review of particle physics. *Prog. Theor. Exp. Phys.* **2020**, 083C01 (2020). <https://doi.org/10.1093/ptep/ptaa104>
- ATLAS Collaboration, Jet reconstruction and performance using particle flow with the ATLAS detector. *Eur. Phys. J. C* **77**, 466 (2017). <https://doi.org/10.1140/epjc/s10052-017-5031-2>. [arXiv:1703.10485](https://arxiv.org/abs/1703.10485) [hep-ex]
- ATLAS Collaboration, Jet energy scale and resolution measured in proton–proton collisions at $\sqrt{s} = 13$ TeV with the ATLAS detector (2020). [arXiv:2007.02645](https://arxiv.org/abs/2007.02645) [hep-ex]
- ATLAS Collaboration, Variable radius, exclusive- k_T , and center-of-mass subjet reconstruction for Higgs($\rightarrow b\bar{b}$) tagging in ATLAS. ATLAS-PHYS-PUB-2017-010 (2017). <https://cds.cern.ch/record/2268678>
- ATLAS Collaboration, ATLAS insertable B-layer technical design report. ATLAS-TDR-19; CERN-LHCC-2010-013 (2010). <https://cds.cern.ch/record/1291633> [Addendum: ATLAS-TDR-19-ADD-1; CERN-LHCC-2012-009 (2012). <https://cds.cern.ch/record/1451888>]
- B. Abbott et al., Production and integration of the ATLAS insertable B-layer. *JINST* **13**, T05008 (2018). <https://doi.org/10.1088/1748-0221/13/05/T05008>. [arXiv:1803.00844](https://arxiv.org/abs/1803.00844) [physics.ins-det]
- ATLAS Collaboration, Performance of the ATLAS trigger system in 2015. *Eur. Phys. J. C* **77**, 317 (2017). <https://doi.org/10.1140/epjc/s10052-017-4852-3>. [arXiv:1611.09661](https://arxiv.org/abs/1611.09661) [hep-ex]
- ATLAS Collaboration, The ATLAS collaboration software and firmware. ATLAS-SOFT-PUB-2021-001 (2021). <https://cds.cern.ch/record/2767187>
- ATLAS Collaboration, Luminosity determination in pp collisions at $\sqrt{s} = 13$ TeV using the ATLAS detector at the LHC. ATLAS-CONF-2019-021 (2019). <https://cds.cern.ch/record/2677054>
- G. Avoni et al., The new LUCID-2 detector for luminosity measurement and monitoring in ATLAS. *JINST* **13**, P07017 (2018). <https://doi.org/10.1088/1748-0221/13/07/P07017>
- ATLAS Collaboration, Performance of electron and photon triggers in ATLAS during LHC Run 2. *Eur. Phys. J. C* **80**, 47 (2020). <https://doi.org/10.1140/epjc/s10052-019-7500-2>. [arXiv:1909.00761](https://arxiv.org/abs/1909.00761) [hep-ex]
- ATLAS Collaboration, Performance of the ATLAS muon triggers in Run 2. *JINST* **15**, P09015 (2020). <https://doi.org/10.1088/1748-0221/15/09/p09015>. [arXiv:2004.13447](https://arxiv.org/abs/2004.13447) [hep-ex]
- ATLAS Collaboration, The ATLAS simulation infrastructure. *Eur. Phys. J. C* **70**, 823 (2010). <https://doi.org/10.1140/epjc/s10052-010-1429-9>. [arXiv:1005.4568](https://arxiv.org/abs/1005.4568) [physics.ins-det]
- GEANT4 Collaboration, S. Agostinelli et al., GEANT4—a simulation toolkit. *Nucl. Instrum. Methods A* **506**, 250 (2003). [https://doi.org/10.1016/S0168-9002\(03\)01368-8](https://doi.org/10.1016/S0168-9002(03)01368-8)
- T. Sjöstrand et al., An introduction to PYTHIA 8.2. *Comput. Phys. Commun.* **191**, 159 (2015). <https://doi.org/10.1016/j.cpc.2015.01.024>. [arXiv:1410.3012](https://arxiv.org/abs/1410.3012) [hep-ph]
- R.D. Ball et al., Parton distributions for the LHC run II. *JHEP* **04**, 040 (2015). [https://doi.org/10.1007/JHEP04\(2015\)040](https://doi.org/10.1007/JHEP04(2015)040). [arXiv:1410.8849](https://arxiv.org/abs/1410.8849) [hep-ph]
- R.D. Ball et al., Parton distributions with LHC data. *Nucl. Phys. B* **867**, 244 (2013). <https://doi.org/10.1016/j.nuclphysb.2012.10.003>. [arXiv:1207.1303](https://arxiv.org/abs/1207.1303) [hep-ph]
- ATLAS Collaboration, The Pythia 8 A3 tune description of ATLAS minimum bias and inelastic measurements incorporating the Donnachie–Landshoff diffractive model. ATLAS-PHYS-PUB-2016-017 (2016). <https://cds.cern.ch/record/2206965>
- E. Bothmann et al., Event generation with Sherpa 2.2. *SciPost Phys.* **7**, 034 (2019). <https://doi.org/10.21468/SciPostPhys.7.3.034>. [arXiv:1905.09127](https://arxiv.org/abs/1905.09127) [hep-ph]
- D.J. Lange, The EvtGen particle decay simulation package. *Nucl. Instrum. Methods A* **462**, 152 (2001). [https://doi.org/10.1016/S0168-9002\(01\)00089-4](https://doi.org/10.1016/S0168-9002(01)00089-4)
- S. Frixione, P. Nason, G. Ridolfi, A positive-weight next-to-leading-order Monte Carlo for heavy flavour hadroproduction. *JHEP* **09**, 126 (2007). <https://doi.org/10.1088/1126-6708/2007/09/126>. [arXiv:0707.3088](https://arxiv.org/abs/0707.3088) [hep-ph]

34. P. Nason, A new method for combining NLO QCD with shower Monte Carlo algorithms. *JHEP* **11**, 040 (2004). <https://doi.org/10.1088/1126-6708/2004/11/040>. [arXiv:hep-ph/0409146](https://arxiv.org/abs/hep-ph/0409146)
35. S. Frixione, P. Nason, C. Oleari, Matching NLO QCD computations with Parton Shower simulations: the POWHEG method. *JHEP* **11**, 070 (2007). <https://doi.org/10.1088/1126-6708/2007/11/070>. [arXiv:0709.2092](https://arxiv.org/abs/0709.2092) [hep-ph]
36. S. Alioli, P. Nason, C. Oleari, E. Re, A general framework for implementing NLO calculations in shower Monte Carlo programs: the POWHEG BOX. *JHEP* **06**, 043 (2010). [https://doi.org/10.1007/JHEP06\(2010\)043](https://doi.org/10.1007/JHEP06(2010)043). [arXiv:1002.2581](https://arxiv.org/abs/1002.2581) [hep-ph]
37. ATLAS Collaboration, Studies on top-quark Monte Carlo modelling for Top2016. ATL-PHYS-PUB-2016-020 (2016). <https://cds.cern.ch/record/2216168>
38. ATLAS Collaboration, Studies on top-quark Monte Carlo modelling with Sherpa and MG5_aMC@NLO. ATL-PHYS-PUB-2017-007 (2017). <https://cds.cern.ch/record/2261938>
39. M. Bähr et al., Herwig++ physics and manual. *Eur. Phys. J. C* **58**, 639 (2008). <https://doi.org/10.1140/epjc/s10052-008-0798-9>. [arXiv:0803.0883](https://arxiv.org/abs/0803.0883) [hep-ph]
40. J. Bellm et al., Herwig 7.0/Herwig++ 3.0 release note. *Eur. Phys. J. C* **76**, 196 (2016). <https://doi.org/10.1140/epjc/s10052-016-4018-8>. [arXiv:1512.01178](https://arxiv.org/abs/1512.01178) [hep-ph]
41. L.A. Harland-Lang, A.D. Martin, P. Motylinski, R.S. Thorne, Parton distributions in the LHC era: MMHT 2014 PDFs. *Eur. Phys. J. C* **75**, 204 (2015). <https://doi.org/10.1140/epjc/s10052-015-3397-6>. [arXiv:1412.3989](https://arxiv.org/abs/1412.3989) [hep-ph]
42. S. Frixione, E. Laenen, P. Motylinski, C. White, B.R. Webber, Single-top hadroproduction in association with a W boson. *JHEP* **07**, 029 (2008). <https://doi.org/10.1088/1126-6708/2008/07/029>. [arXiv:0805.3067](https://arxiv.org/abs/0805.3067) [hep-ph]
43. T. Gleisberg, S. Höche, Comix, a new matrix element generator. *JHEP* **12**, 039 (2008). <https://doi.org/10.1088/1126-6708/2008/12/039>. [arXiv:0808.3674](https://arxiv.org/abs/0808.3674) [hep-ph]
44. F. Buccioni et al., OpenLoops 2. *Eur. Phys. J. C* **79**, 866 (2019). <https://doi.org/10.1140/epjc/s10052-019-7306-2>. [arXiv:1907.13071](https://arxiv.org/abs/1907.13071) [hep-ph]
45. F. Cascioli, P. Maierhöfer, S. Pozzorini, Scattering amplitudes with open loops. *Phys. Rev. Lett.* **108**, 111601 (2012). <https://doi.org/10.1103/PhysRevLett.108.111601>. [arXiv:1111.5206](https://arxiv.org/abs/1111.5206) [hep-ph]
46. A. Denner, S. Dittmaier, L. Hofer, COLLIER: a Fortran-based complex one-loop library in extended regularizations. *Comput. Phys. Commun.* **212**, 220 (2017). <https://doi.org/10.1016/j.cpc.2016.10.013>. [arXiv:1604.06792](https://arxiv.org/abs/1604.06792) [hep-ph]
47. S. Schumann, F. Krauss, A parton shower algorithm based on Catani–Seymour dipole factorisation. *JHEP* **03**, 038 (2008). <https://doi.org/10.1088/1126-6708/2008/03/038>. [arXiv:0709.1027](https://arxiv.org/abs/0709.1027) [hep-ph]
48. S. Höche, F. Krauss, M. Schönherr, F. Siegert, A critical appraisal of NLO+PS matching methods. *JHEP* **09**, 049 (2012). [https://doi.org/10.1007/JHEP09\(2012\)049](https://doi.org/10.1007/JHEP09(2012)049). [arXiv:1111.1220](https://arxiv.org/abs/1111.1220) [hep-ph]
49. S. Höche, F. Krauss, M. Schönherr, F. Siegert, QCD matrix elements + parton showers. The NLO case. *JHEP* **04**, 027 (2013). [https://doi.org/10.1007/JHEP04\(2013\)027](https://doi.org/10.1007/JHEP04(2013)027). [arXiv:1207.5030](https://arxiv.org/abs/1207.5030) [hep-ph]
50. S. Catani, F. Krauss, B.R. Webber, R. Kuhn, QCD matrix elements + parton showers. *JHEP* **11**, 063 (2001). <https://doi.org/10.1088/1126-6708/2001/11/063>. [arXiv:hep-ph/0109231](https://arxiv.org/abs/hep-ph/0109231)
51. S. Höche, F. Krauss, S. Schumann, F. Siegert, QCD matrix elements and truncated showers. *JHEP* **05**, 053 (2009). <https://doi.org/10.1088/1126-6708/2009/05/053>. [arXiv:0903.1219](https://arxiv.org/abs/0903.1219) [hep-ph]
52. C. Anastasiou, L.J. Dixon, K. Melnikov, F. Petriello, High-precision QCD at hadron colliders: electroweak gauge boson rapidity distributions at next-to-next-to leading order. *Phys. Rev. D* **69**, 094008 (2004). <https://doi.org/10.1103/PhysRevD.69.094008>. [arXiv:hep-ph/0312266](https://arxiv.org/abs/hep-ph/0312266)
53. J. Alwall et al., The automated computation of tree-level and next-to-leading order differential cross sections, and their matching to parton shower simulations. *JHEP* **07**, 079 (2014). [https://doi.org/10.1007/JHEP07\(2014\)079](https://doi.org/10.1007/JHEP07(2014)079). [arXiv:1405.0301](https://arxiv.org/abs/1405.0301) [hep-ph]
54. ATLAS Collaboration, Electron and photon performance measurements with the ATLAS detector using the 2015–2017 LHC proton–proton collision data. *JINST* **14**, P12006 (2019). <https://doi.org/10.1088/1748-0221/14/12/P12006>. [arXiv:1908.00005](https://arxiv.org/abs/1908.00005) [hep-ex]
55. ATLAS Collaboration, Muon reconstruction and identification efficiency in ATLAS using the full Run 2 pp collision data set at $\sqrt{s} = 13$ TeV. *Eur. Phys. J. C* **81**, 578 (2021). <https://doi.org/10.1140/epjc/s10052-021-09233-2>. [arXiv:2012.00578](https://arxiv.org/abs/2012.00578) [hep-ex]
56. ATLAS Collaboration, Muon reconstruction and identification efficiency in ATLAS using the full Run 2 pp collision data set at $\sqrt{s} = 13$ TeV (2020). [arXiv:2012.00578](https://arxiv.org/abs/2012.00578) [hep-ex]
57. M. Cacciari, G.P. Salam, G. Soyez, The anti- k_r jet clustering algorithm. *JHEP* **04**, 063 (2008). <https://doi.org/10.1088/1126-6708/2008/04/063>. [arXiv:0802.1189](https://arxiv.org/abs/0802.1189) [hep-ph]
58. M. Cacciari, G.P. Salam, G. Soyez, FastJet user manual. *Eur. Phys. J. C* **72**, 1896 (2012). <https://doi.org/10.1140/epjc/s10052-012-1896-2>. [arXiv:1111.6097](https://arxiv.org/abs/1111.6097) [hep-ph]
59. ATLAS Collaboration, Performance of pile-up mitigation techniques for jets in pp collisions at $\sqrt{s} = 8$ TeV using the ATLAS detector. *Eur. Phys. J. C* **76**, 581 (2016). <https://doi.org/10.1140/epjc/s10052-016-4395-z>. [arXiv:1510.03823](https://arxiv.org/abs/1510.03823) [hep-ex]
60. ATLAS Collaboration, Measurements of top-quark pair differential and double-differential cross-sections in the ℓ +jets channel with pp collisions at $\sqrt{s} = 13$ TeV using the ATLAS detector. *Eur. Phys. J. C* **79**, 1028 (2019). <https://doi.org/10.1140/epjc/s10052-019-7525-6>. [arXiv:1908.07305](https://arxiv.org/abs/1908.07305) [hep-ex] [Erratum: *Eur. Phys. J. C* **80**, 1092 (2020)]
61. ATLAS Collaboration, Performance of missing transverse momentum reconstruction with the ATLAS detector using proton–proton collisions at $\sqrt{s} = 13$ TeV. *Eur. Phys. J. C* **78**, 903 (2018). <https://doi.org/10.1140/epjc/s10052-018-6288-9>. [arXiv:1802.08168](https://arxiv.org/abs/1802.08168) [hep-ex]
62. ATLAS Collaboration, Optimisation and performance studies of the ATLAS b -tagging algorithms for the 2017–18 LHC run. ATL-PHYS-PUB-2017-013 (2017). <https://cds.cern.ch/record/2273281>
63. J. Erdmann et al., A likelihood-based reconstruction algorithm for top-quark pairs and the KLfitter framework. *Nucl. Instrum. Methods A* **748**, 18 (2014). <https://doi.org/10.1016/j.nima.2014.02.029>. ISSN:0168-9002
64. ATLAS Collaboration, Measurements of inclusive and differential fiducial cross-sections of $t\bar{t}$ production with additional heavy-flavour jets in proton–proton collisions at $\sqrt{s} = 13$ TeV with the ATLAS detector. *JHEP* **04**, 046 (2019). [https://doi.org/10.1007/JHEP04\(2019\)046](https://doi.org/10.1007/JHEP04(2019)046). [arXiv:1811.12113](https://arxiv.org/abs/1811.12113) [hep-ex]
65. ATLAS Collaboration, E_T^{miss} performance in the ATLAS detector using 2015–2016 LHC pp collisions. ATL-CONF-2018-023 (2018). <https://cds.cern.ch/record/2625233>
66. ATLAS Collaboration, Forward jet vertex tagging using the particle flow algorithm. ATL-PHYS-PUB-2019-026 (2019). <https://cds.cern.ch/record/2683100>
67. ATLAS Collaboration, ATLAS computing acknowledgements. ATL-SOFT-PUB-2021-003. <https://cds.cern.ch/record/2776662>

ATLAS Collaboration

G. Aad⁹⁸, B. Abbott¹²³, D. C. Abbott⁹⁹, A. Abed Abud³⁴, K. Abeling⁵¹, D. K. Abhayasinghe⁹¹, S. H. Abidi²⁷, A. Aboulhorma^{33c}, H. Abramowicz¹⁵⁶, H. Abreu¹⁵⁵, Y. Abulaiti⁵, A. C. Abusleme Hoffman^{141a}, B. S. Acharya^{64a,64b,o}, B. Achkar⁵¹, L. Adam⁹⁶, C. Adam Bourdarios⁴, L. Adamczyk^{81a}, L. Adamek¹⁶¹, S. V. Addepalli²⁴, J. Adelman¹¹⁶, A. Adiguzel^{11c,ac}, S. Adorni⁵², T. Adye¹³⁸, A. A. Affolder¹⁴⁰, Y. Afik³⁴, C. Agapopoulou⁶², M. N. Agaras¹², J. Agarwala^{68a,68b}, A. Aggarwal¹¹⁴, C. Agheorghiesei^{25c}, J. A. Aguilar-Saavedra^{134a,134f,ab}, A. Ahmad³⁴, F. Ahmadov⁷⁷, W. S. Ahmed¹⁰⁰, X. Ai⁴⁴, G. Aielli^{71a,71b}, I. Aizenberg¹⁷⁴, S. Akatsuka⁸³, M. Akbiyik⁹⁶, T. P. A. Åkesson⁹⁴, A. V. Akimov¹⁰⁷, K. Al Khoury³⁷, G. L. Alberghi^{21b}, J. Albert¹⁷⁰, P. Albicocco⁴⁹, M. J. Alconada Verzini⁸⁶, S. Alderweireldt⁴⁸, M. Aleksa³⁴, I. N. Aleksandrov⁷⁷, C. Alexa^{25b}, T. Alexopoulos⁹, A. Alfonsi¹¹⁵, F. Alfonsi^{21b}, M. Alhroob¹²³, B. Ali¹³⁶, S. Ali¹⁵³, M. Aliev¹⁶⁰, G. Alimonti^{66a}, C. Allaire³⁴, B. M. M. Allbrooke¹⁵¹, P. P. Allport¹⁹, A. Aloisio^{67a,67b}, F. Alonso⁸⁶, C. Alpigiani¹⁴³, E. Alunno Camelia^{71a,71b}, M. Alvarez Estevez⁹⁵, M. G. Alvigi^{67a,67b}, Y. Amaral Coutinho^{78b}, A. Ambler¹⁰⁰, L. Ambroz¹²⁹, C. Amelung³⁴, D. Amidei¹⁰², S. P. Amor Dos Santos^{134a}, S. Amoroso⁴⁴, K. R. Amos¹⁶⁸, C. S. Amrouche⁵², V. Ananiev¹²⁸, C. Anastopoulos¹⁴⁴, N. Andari¹³⁹, T. Andeen¹⁰, J. K. Anders¹⁸, S. Y. Andreev^{43a,43b}, A. Andreatta^{66a,66b}, S. Angelidakis⁸, A. Angerami³⁷, A. V. Anisenkov^{117a,117b}, A. Annovi^{69a}, C. Antel⁵², M. T. Anthony¹⁴⁴, E. Antipov¹²⁴, M. Antonelli⁴⁹, D. J. A. Antrim¹⁶, F. Anulli^{70a}, M. Aoki⁷⁹, J. A. Aparisi Pozo¹⁶⁸, M. A. Aparo¹⁵¹, L. Aperio Bella⁴⁴, N. Aranzabal³⁴, V. Araujo Ferraz^{78a}, C. Arcangeletti⁴⁹, A. T. H. Arce⁴⁷, E. Arena⁸⁸, J.-F. Arguin¹⁰⁶, S. Argyropoulos⁵⁰, J.-H. Arling⁴⁴, A. J. Armbruster³⁴, A. Armstrong¹⁶⁵, O. Arnaez¹⁶¹, H. Arnold³⁴, Z. P. Arrubarrena Tame¹¹⁰, G. Artoni¹²⁹, H. Asada¹¹², K. Asai¹²¹, S. Asai¹⁵⁸, N. A. Asbah⁵⁷, E. M. Asimakopoulou¹⁶⁶, L. Asquith¹⁵¹, J. Assahsah^{33d}, K. Assamagan²⁷, R. Astalos^{26a}, R. J. Atkin^{31a}, M. Atkinson¹⁶⁷, N. B. Atlay¹⁷, H. Atmani^{58b}, P. A. Atlasiddha¹⁰², K. Augsten¹³⁶, S. Auricchio^{67a,67b}, V. A. Austrup¹⁷⁶, G. Avner¹⁵⁵, G. Avolio³⁴, M. K. Ayoub^{13c}, G. Azuelos^{106,ai}, D. Babal^{26a}, H. Bachacou¹³⁹, K. Bachas¹⁵⁷, A. Bachi³², F. Backman^{43a,43b}, A. Badea⁵⁷, P. Bagnaia^{70a,70b}, H. Bahrasemani¹⁴⁷, A. J. Bailey¹⁶⁸, V. R. Bailey¹⁶⁷, J. T. Baines¹³⁸, C. Bakalis⁹, O. K. Baker¹⁷⁷, P. J. Bakker¹¹⁵, E. Bakos¹⁴, D. Bakshi Gupta⁷, S. Balaji¹⁵², R. Balasubramanian¹¹⁵, E. M. Baldin^{117a,117b}, P. Balek¹³⁷, E. Ballabene^{66a,66b}, F. Balli¹³⁹, L. M. Baltes^{59a}, W. K. Balunas¹²⁹, J. Balz⁹⁶, E. Banas⁸², M. Bandieramonte¹³³, A. Bandyopadhyay²², S. Bansal²², L. Barak¹⁵⁶, E. L. Barberio¹⁰¹, D. Barberis^{53a,53b}, M. Barbero⁹⁸, G. Barbour⁹², K. N. Barends^{31a}, T. Barillari¹¹¹, M.-S. Barisits³⁴, J. Barkeloo¹²⁶, T. Barklow¹⁴⁸, B. M. Barnett¹³⁸, R. M. Barnett¹⁶, A. Baroncelli^{58a}, G. Barone²⁷, A. J. Barr¹²⁹, L. Barranco Navarro^{43a,43b}, F. Barreiro⁹⁵, J. Barreiro Guimarães da Costa^{13a}, U. Barron¹⁵⁶, S. Barsov¹³², F. Bartels^{59a}, R. Bartoldus¹⁴⁸, G. Bartolini⁹⁸, A. E. Barton⁸⁷, P. Bartos^{26a}, A. Basalae⁴⁴, A. Basan⁹⁶, M. Baselga⁴⁴, I. Bashta^{72a,72b}, A. Bassalat⁶², M. J. Basso¹⁶¹, C. R. Basson⁹⁷, R. L. Bates⁵⁵, S. Batlamous^{33c}, J. R. Batley³⁰, B. Batool¹⁴⁶, M. Battaglia¹⁴⁰, M. Baucé^{70a,70b}, F. Bauer^{139,*}, P. Bauer²², H. S. Bawa²⁹, A. Bayirli^{11c}, J. B. Beacham⁴⁷, T. Beau¹³⁰, P. H. Beauchemin¹⁶⁴, F. Becherer⁵⁰, P. Bechtel²², H. P. Beck^{18,q}, K. Becker¹⁷², C. Becot⁴⁴, A. J. Beddall^{11a}, V. A. Bednyakov⁷⁷, C. P. Bee¹⁵⁰, T. A. Beermann³⁴, M. Begalli^{78b}, M. Begel²⁷, A. Behera¹⁵⁰, J. K. Behr⁴⁴, C. Beirao Da Cruz E Silva³⁴, J. F. Beirer^{34,51}, F. Beisiegel²², M. Belfkir⁴, G. Bella¹⁵⁶, L. Bellagamba^{21b}, A. Bellerive³², P. Bellos¹⁹, K. Beloborodov^{117a,117b}, K. Belotskiy¹⁰⁸, N. L. Belyaev¹⁰⁸, D. Benckekroun^{33a}, Y. Benhammou¹⁵⁶, D. P. Benjamin²⁷, M. Benoit²⁷, J. R. Bensinger²⁴, S. Bentvelsen¹¹⁵, L. Beresford³⁴, M. Beretta⁴⁹, D. Berge¹⁷, E. Bergeas Kuutmann¹⁶⁶, N. Berger⁴, B. Bergmann¹³⁶, L. J. Bergsten²⁴, J. Beringer¹⁶, S. Berlendis⁶, G. Bernardi¹³⁰, C. Bernius¹⁴⁸, F. U. Bernlochner²², T. Berry⁹¹, P. Berta¹³⁷, A. Berthold⁴⁶, I. A. Bertram⁸⁷, O. Bessidskaia Bylund¹⁷⁶, S. Bethke¹¹¹, A. Betti⁴⁰, A. J. Bevan⁹⁰, S. Bhatta¹⁵⁰, D. S. Bhattacharya¹⁷¹, P. Bhattarai²⁴, V. S. Bhopatkar⁵, R. Bi¹³³, R. Bi²⁷, R. M. Bianchi¹³³, O. Biebel¹¹⁰, R. Bielski¹²⁶, N. V. Biesuz^{69a,69b}, M. Biglietti^{72a}, T. R. V. Billoud¹³⁶, M. Bindi⁵¹, A. Bingul^{11d}, C. Bini^{70a,70b}, S. Biondi^{21a,21b}, A. Biondini⁸⁸, C. J. Birch-sykes⁹⁷, G. A. Bird^{19,139}, M. Birman¹⁷⁴, T. Bisanz³⁴, J. P. Biswal², D. Biswas^{175,j}, A. Bitadze⁹⁷, C. Bittrich⁴⁶, K. Björke¹²⁸, I. Bloch⁴⁴, C. Blocker²⁴, A. Blue⁵⁵, U. Blumenschein⁹⁰, J. Blumenthal⁹⁶, G. J. Bobbink¹¹⁵, V. S. Bobrovnikov^{117a,117b}, M. Boehler⁵⁰, D. Bogavac¹², A. G. Bogdanchikov^{117a,117b}, C. Bohm^{43a}, V. Boisvert⁹¹, P. Bokan⁴⁴, T. Bold^{81a}, M. Bomben¹³⁰, M. Bona⁹⁰, M. Boonekamp¹³⁹, C. D. Booth⁹¹, A. G. Borbély⁵⁵, H. M. Borecka-Bielska¹⁰⁶, L. S. Borgna⁹², G. Borissov⁸⁷, D. Bortoletto¹²⁹, D. Boscherini^{21b}, M. Bosman¹², J. D. Bossio Sola³⁴, K. Bouaouda^{33a}, J. Boudreau¹³³, E. V. Bouhova-Thacker⁸⁷, D. Boumediene³⁶, R. Bouquet¹³⁰, A. Boveia¹²²

J. Boyd³⁴, D. Boye²⁷, I. R. Boyko⁷⁷, A. J. Bozson⁹¹, J. Bracik¹⁹, N. Brahimi^{58c,58d}, G. Brandt¹⁷⁶, O. Brandt³⁰, F. Braren⁴⁴, B. Brau⁹⁹, J. E. Brau¹²⁶, W. D. Breaden Madden⁵⁵, K. Brendlinger⁴⁴, R. Brenner¹⁷⁴, L. Brenner³⁴, R. Brenner¹⁶⁶, S. Bressler¹⁷⁴, B. Brickwedde⁹⁶, D. L. Briglin¹⁹, D. Britton⁵⁵, D. Britzger¹¹¹, I. Brock²², R. Brock¹⁰³, G. Brooijmans³⁷, W. K. Brooks^{141f}, E. Brost²⁷, P. A. Bruckman de Renstrom⁸², B. Brüers⁴⁴, D. Bruncko^{26b}, A. Bruni^{21b}, G. Bruni^{21b}, M. Bruschi^{21b}, N. Bruscinò^{70a,70b}, L. Bryngemark¹⁴⁸, T. Buanes¹⁵, Q. Buat¹⁵⁰, P. Buchholz¹⁴⁶, A. G. Buckley⁵⁵, I. A. Budagov⁷⁷, M. K. Bugge¹²⁸, O. Bulekov¹⁰⁸, B. A. Bullard⁵⁷, S. Burdin⁸⁸, C. D. Burgard⁴⁴, A. M. Burger¹²⁴, B. Burghgrave⁷, J. T. P. Burr³⁰, C. D. Burton¹⁰, J. C. Burzynski¹⁴⁷, E. L. Busch³⁷, V. Büscher⁹⁶, P. J. Bussey⁵⁵, J. M. Butler²³, C. M. Buttar⁵⁵, J. M. Butterworth⁹², W. Buttinger¹³⁸, C. J. Buxo Vazquez¹⁰³, A. R. Buzykaev^{117a,117b}, G. Cabras^{21b}, S. Cabrera Urbán¹⁶⁸, D. Caforio⁵⁴, H. Cai¹³³, V. M. M. Cairo¹⁴⁸, O. Kakir^{3a}, N. Calace³⁴, P. Calafiura¹⁶, G. Calderini¹³⁰, P. Calfayan⁶³, G. Callea⁵⁵, L. P. Caloba^{78b}, D. Calvet³⁶, S. Calvet³⁶, T. P. Calvet⁹⁸, M. Calvetti^{69a,69b}, R. Camacho Toro¹³⁰, S. Camarda³⁴, D. Camarero Munoz⁹⁵, P. Camarri^{71a,71b}, M. T. Camerlingo^{72a,72b}, D. Cameron¹²⁸, C. Camincher¹⁷⁰, M. Campanelli⁹², A. Camplani³⁸, V. Canale^{67a,67b}, A. Canesse¹⁰⁰, M. Cano Bret⁷⁵, J. Cantero¹²⁴, Y. Cao¹⁶⁷, F. Capocasa²⁴, M. Capua^{39a,39b}, A. Carbone^{66a,66b}, R. Cardarelli^{71a}, J. C. J. Cardenas⁷, F. Cardillo¹⁶⁸, G. Carducci^{39a,39b}, T. Carli³⁴, G. Carlino^{67a}, B. T. Carlson¹³³, E. M. Carlson^{162a,170}, L. Carminati^{66a,66b}, M. Carnesale^{70a,70b}, R. M. D. Carney¹⁴⁸, S. Caron¹¹⁴, E. Carquin^{141f}, S. Carrá⁴⁴, G. Carratta^{21a,21b}, J. W. S. Carter¹⁶¹, T. M. Carter⁴⁸, D. Casadei^{31c}, M. P. Casado^{12g}, A. F. Casha¹⁶¹, E. G. Castiglia¹⁷⁷, F. L. Castillo^{59a}, L. Castillo Garcia¹², V. Castillo Gimenez¹⁶⁸, N. F. Castro^{134a,134c}, A. Catinaccio³⁴, J. R. Catmore¹²⁸, A. Cattai³⁴, V. Cavaliere²⁷, N. Cavalli^{21a,21b}, V. Cavasinni^{69a,69b}, E. Celebi^{11b}, F. Celli¹²⁹, M. S. Centonze^{65a,65b}, K. Cerny¹²⁵, A. S. Cerqueira^{78a}, A. Cerri¹⁵¹, L. Cerrito^{71a,71b}, F. Cerutti¹⁶, A. Cervelli^{21b}, S. A. Cetin^{11b}, Z. Chadi^{33a}, D. Chakraborty¹¹⁶, M. Chala^{134f}, J. Chan¹⁷⁵, W. S. Chan¹¹⁵, W. Y. Chan⁸⁸, J. D. Chapman³⁰, B. Chargeishvili^{154b}, D. G. Charlton¹⁹, T. P. Charman⁹⁰, M. Chatterjee¹⁸, S. Chekanov⁵, S. V. Chekulaev^{162a}, G. A. Chelkov^{77,ae}, A. Chen¹⁰², B. Chen¹⁵⁶, B. Chen¹⁷⁰, C. Chen^{58a}, C. H. Chen⁷⁶, H. Chen^{13c}, H. Chen²⁷, J. Chen^{58c}, J. Chen²⁴, S. Chen¹³¹, S. J. Chen^{13c}, X. Chen^{58c}, X. Chen^{13b}, Y. Chen^{58a}, Y.-H. Chen⁴⁴, C. L. Cheng¹⁷⁵, H. C. Cheng^{60a}, A. Cheplakov⁷⁷, E. Cheremushkina⁴⁴, E. Cherepanova⁷⁷, R. Cherkaoui El Moursli^{33e}, E. Cheu⁶, K. Cheung⁶¹, L. Chevalier¹³⁹, V. Chiarella⁴⁹, G. Chiarelli^{69a}, G. Chiodini^{65a}, A. S. Chisholm¹⁹, A. Chitan^{25b}, Y. H. Chiu¹⁷⁰, M. V. Chizhov^{77,s}, K. Choi¹⁰, A. R. Chomont^{70a,70b}, Y. Chou⁹⁹, Y. S. Chow¹¹⁵, T. Chowdhury^{31g}, L. D. Christopher^{31g}, M. C. Chu^{60a}, X. Chu^{13a,13d}, J. Chudoba¹³⁵, J. J. Chwastowski⁸², D. Cieri¹¹¹, K. M. Ciesla⁸², V. Cindro⁸⁹, I. A. Cioara^{25b}, A. Ciocio¹⁶, F. Ciotto^{67a,67b}, Z. H. Citron^{174,k}, M. Citterio^{66a}, D. A. Ciubotaru^{25b}, B. M. Ciungu¹⁶¹, A. Clark⁵², P. J. Clark⁴⁸, J. M. Clavijo Columbie⁴⁴, S. E. Clawson⁹⁷, C. Clement^{43a,43b}, L. Clissa^{21a,21b}, Y. Coadou⁹⁸, M. Cobal^{164a,164c}, A. Coccaro^{53b}, J. Cochran⁷⁶, R. F. Coelho Barrue^{134a}, R. Coelho Lopes De Sa⁹⁹, S. Coelli^{66a}, H. Cohen¹⁵⁶, A. E. C. Coimbra³⁴, B. Cole³⁷, J. Collot⁵⁶, P. Conde Muñio^{134a,134g}, S. H. Connell^{31c}, I. A. Connelly⁵⁵, E. I. Conroy¹²⁹, F. Conventi^{67a,aj}, H. G. Cooke¹⁹, A. M. Cooper-Sarkar¹²⁹, F. Cormier¹⁶⁹, L. D. Corpe³⁴, M. Corradi^{70a,70b}, E. E. Corrigan⁹⁴, F. Corriveau^{100,y}, M. J. Costa¹⁶⁸, F. Costanza⁴, D. Costanzo¹⁴⁴, B. M. Cote¹²², G. Cowan⁹¹, J. W. Cowley³⁰, K. Cranmer¹²⁰, S. Crépe-Renaudin⁵⁶, F. Crescioli¹³⁰, M. Cristinziani¹⁴⁶, M. Cristoforetti^{73a,73b,b}, V. Croft¹⁶⁴, G. Crosetti^{39a,39b}, A. Cueto³⁴, T. Cuhadar Donszelmann¹⁶⁵, H. Cui^{13a,13d}, A. R. Cukierman¹⁴⁸, W. R. Cunningham⁵⁵, F. Curcio^{39a,39b}, P. Czodrowski³⁴, M. M. Czurylo^{59b}, M. J. Da Cunha Sargedas De Sousa^{58a}, J. V. Da Fonseca Pinto^{78b}, C. Da Via⁹⁷, W. Dabrowski^{81a}, T. Dado⁴⁵, S. Dahbi^{31g}, T. Dai¹⁰², C. Dallapiccola⁹⁹, M. Dam³⁸, G. D'amen²⁷, V. D'Amico^{72a,72b}, J. Damp⁹⁶, J. R. Dandoy¹³¹, M. F. Daneri²⁸, M. Danninger¹⁴⁷, V. Dao³⁴, G. Darbo^{53b}, S. Darmora⁵, A. Dattagupta¹²⁶, S. D'Auria^{66a,66b}, C. David^{162b}, T. Davidek¹³⁷, D. R. Davis⁴⁷, B. Davis-Purcell³², I. Dawson⁹⁰, K. De⁷, R. De Asmundis^{67a}, M. De Beurs¹¹⁵, S. De Castro^{21a,21b}, N. De Groot¹¹⁴, P. de Jong¹¹⁵, H. De la Torre¹⁰³, A. De Maria^{13c}, D. De Pedis^{70a}, A. De Salvo^{70a}, U. De Sanctis^{71a,71b}, M. De Santis^{71a,71b}, A. De Santo¹⁵¹, J. B. De Vivie De Regie⁵⁶, D. V. Dedovich⁷⁷, J. Degens¹¹⁵, A. M. Deiana⁴⁰, J. Del Peso⁹⁵, Y. Delabat Diaz⁴⁴, F. Deliot¹³⁹, C. M. Delitzsch⁶, M. Della Pietra^{67a,67b}, D. Della Volpe⁵², A. Dell'Acqua³⁴, L. Dell'Asta^{66a,66b}, M. Delmastro⁴, P. A. Delsart⁵⁶, S. Demers¹⁷⁷, M. Demichev⁷⁷, S. P. Denisov¹¹⁸, L. D'Eramo¹¹⁶, D. Derendarz⁸², J. E. Derkaoui^{33d}, F. Derue¹³⁰, P. Dervan⁸⁸, K. Desch²², K. Dette¹⁶¹, C. Deutsch²², P. O. Deviveiros³⁴, F. A. Di Bello^{70a,70b}, A. Di Ciaccio^{71a,71b}, L. Di Ciaccio⁴, A. Di Domenico^{70a,70b}, C. Di Donato^{67a,67b}, A. Di Girolamo³⁴, G. Di Gregorio^{69a,69b}, A. Di Luca^{73a,73b,b}, B. Di Micco^{72a,72b}, R. Di Nardo^{72a,72b}, C. Diaconu⁹⁸, F. A. Dias¹¹⁵, T. Dias Do Vale^{134a}, M. A. Diaz^{141a}, F. G. Diaz Capriles²²,

J. Dickinson¹⁶, M. Didenko¹⁶⁸, E. B. Diehl¹⁰², J. Dietrich¹⁷, S. Díez Cornell⁴⁴, C. Díez Pardos¹⁴⁶, A. Dimitrievska¹⁶, W. Ding^{13b}, J. Dingfelder²², I-M. Dinu^{25b}, S. J. Dittmeier^{59b}, F. Dittus³⁴, F. Djama⁹⁸, T. Djobava^{154b}, J. I. Djuvsland¹⁵, M. A. B. Do Vale¹⁴², D. Dodsworth²⁴, C. Doglioni⁹⁴, J. Dolejsi¹³⁷, Z. Dolezal¹³⁷, M. Donadelli^{78c}, B. Dong^{58c}, J. Donini³⁶, A. D'Onofrio^{13c}, M. D'Onofrio⁸⁸, J. Dopke¹³⁸, A. Doria^{67a}, M. T. Dova⁸⁶, A. T. Doyle⁵⁵, E. Drechsler¹⁴⁷, E. Dreyer¹⁴⁷, T. Dreyer⁵¹, A. S. Drobac¹⁶⁴, D. Du^{58a}, T. A. du Pree¹¹⁵, F. Dubinin¹⁰⁷, M. Dubovsky^{26a}, A. Dubreuil⁵², E. Duchovni¹⁷⁴, G. Duckeck¹¹⁰, O. A. Ducu^{25b,34}, D. Duda¹¹¹, A. Dudarev³⁴, M. D'uffizi⁹⁷, L. Duflo⁶², M. Dührssen³⁴, C. Dülsen¹⁷⁶, A. E. Dumitriu^{25b}, M. Dunford^{59a}, S. Dungs⁴⁵, K. Dunne^{43a,43b}, A. Duperrin⁹⁸, H. Duran Yildiz^{3a}, M. Düren⁵⁴, A. Durglishvili^{154b}, B. Dutta⁴⁴, G. I. Dyckes¹⁶, M. Dyndal^{81a}, S. Dysch⁹⁷, B. S. Dziedzic⁸², B. Eckerova^{26a}, M. G. Eggleston⁴⁷, E. Egidio Purcino De Souza^{78b}, L. F. Ehrke⁵², T. Eifert⁷, G. Eigen¹⁵, K. Einsweiler¹⁶, T. Ekelof¹⁶⁶, Y. El Ghazali^{33b}, H. El Jarrari^{33c}, A. El Moussaouy^{33a}, V. Ellajosyula¹⁶⁶, M. Ellert¹⁶⁶, F. Ellinghaus¹⁷⁶, A. A. Elliot⁹⁰, N. Ellis³⁴, J. Elmsheuser²⁷, M. Elsing³⁴, D. Emelianov¹³⁸, A. Emerman³⁷, Y. Enari¹⁵⁸, J. Erdmann⁴⁵, A. Ereditato¹⁸, P. A. Erland⁸², M. Errenst¹⁷⁶, M. Escalier⁶², C. Escobar¹⁶⁸, O. Estrada Pastor¹⁶⁸, E. Etzion¹⁵⁶, G. Evans^{134a}, H. Evans⁶³, M. O. Evans¹⁵¹, A. Ezhilov¹³², F. Fabbri⁵⁵, L. Fabbri^{21a,21b}, G. Facini¹⁷², V. Fadeyev¹⁴⁰, R. M. Fakhruddinov¹¹⁸, S. Falciano^{70a}, P. J. Falke²², S. Falke³⁴, J. Faltova¹³⁷, Y. Fan^{13a}, Y. Fang^{13a}, Y. Fang^{13a}, G. Fanourakis⁴², M. Fanti^{66a,66b}, M. Faraj^{58c}, A. Farbin⁷, A. Farilla^{72a}, E. M. Farina^{68a,68b}, T. Faroque¹⁰³, S. M. Farrington⁴⁸, P. Farthouat³⁴, F. Fassi^{33c}, D. Fassouliotis⁸, M. Fauci Giannelli^{71a,71b}, W. J. Fawcett³⁰, L. Fayard⁶², O. L. Fedin^{132,p}, G. Fedotov¹³², M. Feickert¹⁶⁷, L. Felgioni⁹⁸, A. Fell¹⁴⁴, C. Feng^{58b}, M. Feng^{13b}, M. J. Fenton¹⁶⁵, A. B. Fenyuk¹¹⁸, S. W. Ferguson⁴¹, J. Ferrando⁴⁴, A. Ferrari¹⁶⁶, P. Ferrari¹¹⁵, R. Ferrari^{68a}, D. Ferrere⁵², C. Ferretti¹⁰², F. Fiedler⁹⁶, A. Filipčić⁸⁹, F. Filthaut¹¹⁴, M. C. N. Fiolhais^{134a,134c,a}, L. Fiorini¹⁶⁸, F. Fischer¹⁴⁶, W. C. Fisher¹⁰³, T. Fitschen¹⁹, I. Fleck¹⁴⁶, P. Fleischmann¹⁰², T. Flick¹⁷⁶, B. M. Flierl¹¹⁰, L. Flores¹³¹, M. Flores^{31d}, L. R. Flores Castillo^{60a}, F. M. Follega^{73a,73b}, N. Fomin¹⁵, J. H. Foo¹⁶¹, B. C. Forland⁶³, A. Formica¹³⁹, F. A. Förster¹², A. C. Forti⁹⁷, E. Fortin⁹⁸, M. G. Foti¹²⁹, L. Fountas⁸, D. Fournier⁶², H. Fox⁸⁷, P. Francavilla^{69a,69b}, S. Francescato⁵⁷, M. Franchini^{21a,21b}, S. Franchino^{59a}, D. Francis³⁴, L. Franco⁴, L. Franconi¹⁸, M. Franklin⁵⁷, G. Frattari^{70a,70b}, A. C. Freegard⁹⁰, P. M. Freeman¹⁹, W. S. Freund^{78b}, E. M. Freundlich⁴⁵, D. Froidevaux³⁴, J. A. Frost¹²⁹, Y. Fu^{58a}, M. Fujimoto¹²¹, E. Fullana Torregrosa¹⁶⁸, J. Fuster¹⁶⁸, A. Gabrielli^{21a,21b}, A. Gabrielli³⁴, P. Gadov⁴⁴, G. Gagliardi^{53a,53b}, L. G. Gagnon¹⁶, G. E. Gallardo¹²⁹, E. J. Gallas¹²⁹, B. J. Gallop¹³⁸, R. Gamboa Goni⁹⁰, K. K. Gan¹²², S. Ganguly¹⁵⁸, J. Gao^{58a}, Y. Gao⁴⁸, Y. S. Gao^{29,m}, F. M. Garay Walls^{141a}, C. García¹⁶⁸, J. E. García Navarro¹⁶⁸, J. A. García Pascual^{13a}, M. Garcia-Sciveres¹⁶, R. W. Gardner³⁵, D. Garg⁷⁵, R. B. Garg¹⁴⁸, S. Gargiulo⁵⁰, C. A. Garner¹⁶¹, V. Garonne¹²⁸, S. J. Gasiorowski¹⁴³, P. Gaspar^{78b}, G. Gaudio^{68a}, P. Gauzzi^{70a,70b}, I. L. Gavrilenko¹⁰⁷, A. Gavrilyuk¹¹⁹, C. Gay¹⁶⁹, G. Gaycken⁴⁴, E. N. Gazis⁹, A. A. Geanta^{25b}, C. M. Gee¹⁴⁰, C. N. P. Gee¹³⁸, J. Geisen⁹⁴, M. Geisen⁹⁶, C. Gemme^{53b}, M. H. Genest⁵⁶, S. Gentile^{70a,70b}, S. George⁹¹, W. F. George¹⁹, T. Gerialis⁴², L. O. Gerlach⁵¹, P. Gessinger-Befurt³⁴, M. Ghasemi Bostanabad¹⁷⁰, A. Ghosh¹⁶⁵, A. Ghosh⁷⁵, B. Giacobbe^{21b}, S. Giagu^{70a,70b}, N. Giangiacomi¹⁶¹, P. Giannetti^{69a}, A. Giannini^{67a,67b}, S. M. Gibson⁹¹, M. Gignac¹⁴⁰, D. T. Gil^{81b}, B. J. Gilbert³⁷, D. Gillberg³², G. Gilles¹¹⁵, N. E. K. Gillwald⁴⁴, D. M. Gingrich^{2,ai}, M. P. Giordani^{64a,64c}, P. F. Giraud¹³⁹, G. Giugliarelli^{64a,64c}, D. Giugni^{66a}, F. Giulia^{71a,71b}, I. Gkialas^{8,h}, P. Gkoutoumis⁹, L. K. Gladilin¹⁰⁹, C. Glasman⁹⁵, G. R. Gledhill¹²⁶, M. Glisic¹²⁶, I. Gnesi^{39b,d}, M. Goblirsch-Kolb²⁴, D. Godin¹⁰⁶, S. Goldfarb¹⁰¹, T. Golling⁵², D. Golubkov¹¹⁸, J. P. Gombas¹⁰³, A. Gomes^{134a,134b}, R. Goncalves Gama⁵¹, R. Gonçalves^{134a,134c}, G. Gonella¹²⁶, L. Gonella¹⁹, A. Gongadze⁷⁷, F. Gonnella¹⁹, J. L. Gonski³⁷, S. González de la Hoz¹⁶⁸, S. Gonzalez Fernandez¹², R. Gonzalez Lopez⁸⁸, C. Gonzalez Renteria¹⁶, R. Gonzalez Suarez¹⁶⁶, S. Gonzalez-Sevilla⁵², G. R. Gonzalvo Rodriguez¹⁶⁸, R. Y. González Andana^{141a}, L. Goossens³⁴, N. A. Gorasia¹⁹, P. A. Gorbounov¹¹⁹, H. A. Gordon²⁷, B. Gorini³⁴, E. Gorini^{65a,65b}, A. Gorišek⁸⁹, A. T. Goshaw⁴⁷, M. I. Gostkin⁷⁷, C. A. Gottardo¹¹⁴, M. Goughri^{33b}, V. Goumarre⁴⁴, A. G. Goussiou¹⁴³, N. Govender^{31c}, C. Goy⁴, I. Grabowska-Bold^{81a}, K. Graham³², E. Gramstad¹²⁸, S. Grancagnolo¹⁷, M. Grandi¹⁵¹, V. Gratchev¹³², P. M. Gravila^{25f}, F. G. Gravili^{65a,65b}, H. M. Gray¹⁶, C. Grefe²², I. M. Gregor⁴⁴, P. Grenier¹⁴⁸, K. Grevtsov⁴⁴, C. Grieco¹², N. A. Grieser¹²³, A. A. Grillo¹⁴⁰, K. Grimm^{29,1}, S. Grinstein^{12,v}, J.-F. Grivaz⁶², S. Groh⁹⁶, E. Gross¹⁷⁴, J. Grosse-Knetter⁵¹, C. Grud¹⁰², A. Grummer¹¹³, J. C. Grundy¹²⁹, L. Guan¹⁰², W. Guan¹⁷⁵, C. Gubbels¹⁶⁹, J. Guenther³⁴, J. G. R. Guerrero Rojas¹⁶⁸, F. Guescini¹¹¹, D. Guest¹⁷, R. Gugel⁹⁶, A. Guida⁴⁴, T. Guillemain⁴, S. Guindon³⁴, J. Guo^{58c}, L. Guo⁶², Y. Guo¹⁰², R. Gupta⁴⁴, S. Gurbuz²², G. Gustavino¹²³, M. Guth⁵², P. Gutierrez¹²³

L. F. Gutierrez Zagazeta¹³¹, C. Gutsche⁹², C. Guyot¹³⁹, C. Gwenlan¹²⁹, C. B. Gwilliam⁸⁸, E. S. Haaland¹²⁸, A. Haas¹²⁰, M. Habedank⁴⁴, C. Haber¹⁶, H. K. Hadavand⁷, A. Hadeef⁹⁶, S. Hadzic¹¹¹, M. Haleem¹⁷¹, J. Haley¹²⁴, J. J. Hall¹⁴⁴, G. Halladjian¹⁰³, G. D. Hallewell⁹⁸, L. Halser¹⁸, K. Hamano¹⁷⁰, H. Hamdaoui^{33e}, M. Hamer²², G. N. Hamity⁴⁸, K. Han^{58a}, L. Han^{13c}, L. Han^{58a}, S. Han¹⁶, Y. F. Han¹⁶¹, K. Hanagaki^{79,t}, M. Hance¹⁴⁰, M. D. Hank³⁵, R. Hankache⁹⁷, E. Hansen⁹⁴, J. B. Hansen³⁸, J. D. Hansen³⁸, M. C. Hansen²², P. H. Hansen³⁸, K. Hara¹⁶³, T. Harenberg¹⁷⁶, S. Harkusha¹⁰⁴, Y. T. Harris¹²⁹, P. F. Harrison¹⁷², N. M. Hartman¹⁴⁸, N. M. Hartmann¹¹⁰, Y. Hasegawa¹⁴⁵, A. Hasib⁴⁸, S. Hassani¹³⁹, S. Haug¹⁸, R. Hauser¹⁰³, M. Havranek¹³⁶, C. M. Hawkes¹⁹, R. J. Hawkins³⁴, S. Hayashida¹¹², D. Hayden¹⁰³, C. Hayes¹⁰², R. L. Hayes¹⁶⁹, C. P. Hays¹²⁹, J. M. Hays⁹⁰, H. S. Hayward⁸⁸, S. J. Haywood¹³⁸, F. He^{58a}, Y. He¹⁵⁹, Y. He¹³⁰, M. P. Heath⁴⁸, V. Hedberg⁹⁴, A. L. Heggelund¹²⁸, N. D. Hehir⁹⁰, C. Heidegger⁵⁰, K. K. Heidegger⁵⁰, W. D. Heidorn⁷⁶, J. Heilman³², S. Heim⁴⁴, T. Heim¹⁶, B. Heinemann^{44,ag}, J. G. Heinlein¹³¹, J. J. Heinrich¹²⁶, L. Heinrich³⁴, J. Hejbal¹³⁵, L. Helary⁴⁴, A. Held¹²⁰, C. M. Helling¹⁴⁰, S. Hellman^{43a,43b}, C. Helsens³⁴, R. C. W. Henderson⁸⁷, L. Henkelmann³⁰, A. M. Henriques Correia³⁴, H. Herde¹⁴⁸, Y. Hernández Jiménez¹⁵⁰, H. Herr⁹⁶, M. G. Herrmann¹¹⁰, T. Herrmann⁴⁶, G. Herten⁵⁰, R. Hertenberger¹¹⁰, L. Hervás³⁴, N. P. Hessey^{162a}, H. Hibi⁸⁰, S. Higashino⁷⁹, E. Higón-Rodríguez¹⁶⁸, K. H. Hiller⁴⁴, S. J. Hillier¹⁹, M. Hils⁴⁶, I. Hinchliffe¹⁶, F. Hinterkeuser²², M. Hirose¹²⁷, S. Hirose¹⁶³, D. Hirschbuehl¹⁷⁶, B. Hiti⁸⁹, O. Hladik¹³⁵, J. Hobbs¹⁵⁰, R. Hobincu^{25e}, N. Hod¹⁷⁴, M. C. Hodgkinson¹⁴⁴, B. H. Hodgkinson³⁰, A. Hoecker³⁴, J. Hofer⁴⁴, D. Hohn⁵⁰, T. Holm²², T. R. Holmes³⁵, M. Holzbock¹¹¹, L. B. A. H. Hommels³⁰, B. P. Honan⁹⁷, J. Hong^{58c}, T. M. Hong¹³³, Y. Hong⁵¹, J. C. Honig⁵⁰, A. Hönle¹¹¹, B. H. Hooberman¹⁶⁷, W. H. Hopkins⁵, Y. Horii¹¹², L. A. Horyn³⁵, S. Hou¹⁵³, J. Howarth⁵⁵, J. Hoya⁸⁶, M. Hrabovsky¹²⁵, A. Hrynevich¹⁰⁵, T. Hryn'ova⁴, P. J. Hsu⁶¹, S.-C. Hsu¹⁴³, Q. Hu³⁷, S. Hu^{58c}, Y. F. Hu^{13a,13d.ak}, D. P. Huang⁹², X. Huang^{13c}, Y. Huang^{58a}, Y. Huang^{13a}, Z. Hubacek¹³⁶, F. Hubaut⁹⁸, M. Huebner²², F. Huegging²², T. B. Huffman¹²⁹, M. Huhtinen³⁴, S. K. Huiberts¹⁵, R. Hulsken⁵⁶, N. Huseynov^{77,z}, J. Huston¹⁰³, J. Huth⁵⁷, R. Hyneman¹⁴⁸, S. Hyrych^{26a}, G. Iacobucci⁵², G. Iakovidis²⁷, I. Ibragimov¹⁴⁶, L. Iconomidou-Fayard⁶², P. Iengo³⁴, R. Iguchi¹⁵⁸, T. Iizawa⁵², Y. Ikegami⁷⁹, A. Ilg¹⁸, N. Ilic¹⁶¹, H. Imam^{33a}, T. Ingebretsen Carlson^{43a,43b}, G. Introzzi^{68a,68b}, M. Iodice^{72a}, V. Ippolito^{70a,70b}, M. Ishino¹⁵⁸, W. Islam¹⁷⁵, C. Issever^{17,44}, S. Istin^{11c,al}, J. M. Iturbe Ponce^{60a}, R. Iuppa^{73a,73b}, A. Ivina¹⁷⁴, J. M. Izen⁴¹, V. Izzo^{67a}, P. Jacka¹³⁵, P. Jackson¹, R. M. Jacobs⁴⁴, B. P. Jaeger¹⁴⁷, C. S. Jagfeld¹¹⁰, G. Jäkel¹⁷⁶, K. Jakobs⁵⁰, T. Jakoubek¹⁷⁴, J. Jamieson⁵⁵, K. W. Janas^{81a}, G. Jarlskog⁹⁴, A. E. Jaspán⁸⁸, T. Javůrek³⁴, M. Javurkova⁹⁹, F. Jeanneau¹³⁹, L. Jeanty¹²⁶, J. Jejela^{154a,aa}, P. Jenni^{50,e}, S. Jézéquel⁴, J. Jia¹⁵⁰, Z. Jia^{13c}, Y. Jiang^{58a}, S. Jiggins⁴⁸, J. Jimenez Pena¹¹¹, S. Jin^{13c}, A. Jinaru^{25b}, O. Jinnouchi¹⁵⁹, H. Jivan^{31g}, P. Johansson¹⁴⁴, K. A. Johns⁶, C. A. Johnson⁶³, D. M. Jones³⁰, E. Jones¹⁷², R. W. L. Jones⁸⁷, T. J. Jones⁸⁸, J. Jovicevic¹⁴, X. Ju¹⁶, J. J. Junggeburth³⁴, A. Juste Rozas^{12,v}, S. Kabana^{141e}, A. Kaczmarska⁸², M. Kado^{70a,70b}, H. Kagan¹²², M. Kagan¹⁴⁸, A. Kahn³⁷, A. Kahn¹³¹, C. Kahra⁹⁶, T. Kaji¹⁷³, E. Kajomovitz¹⁵⁵, C. W. Kalderon²⁷, A. Kamenshchikov¹¹⁸, M. Kaneda¹⁵⁸, N. J. Kang¹⁴⁰, S. Kang⁷⁶, Y. Kano¹¹², D. Kar^{31g}, K. Karava¹²⁹, M. J. Kareem^{162b}, I. Karkanas¹⁵⁷, S. N. Karpov⁷⁷, Z. M. Karpova⁷⁷, V. Kartvelishvili⁸⁷, A. N. Karyukhin¹¹⁸, E. Kasimi¹⁵⁷, C. Kato^{58d}, J. Katzy⁴⁴, K. Kawade¹⁴⁵, K. Kawagoe⁸⁵, T. Kawaguchi¹¹², T. Kawamoto¹³⁹, G. Kawamura⁵¹, E. F. Kay¹⁷⁰, F. I. Kaya¹⁶⁴, S. Kazakos¹², V. F. Kazanin^{117a,117b}, Y. Ke¹⁵⁰, J. M. Keaveney^{31a}, R. Keeler¹⁷⁰, J. S. Keller³², A. S. Kelly⁹², D. Kelsey¹⁵¹, J. J. Kempster¹⁹, J. Kendrick¹⁹, K. E. Kennedy³⁷, O. Kepka¹³⁵, S. Kersten¹⁷⁶, B. P. Kerševan⁸⁹, S. Ketabchi Haghighat¹⁶¹, M. Khandoga¹³⁰, A. Khanov¹²⁴, A. G. Kharlamov^{117a,117b}, T. Kharlamova^{117a,117b}, E. E. Khoda¹⁴³, T. J. Khoo¹⁷, G. Khorauli¹⁷¹, E. Khramov⁷⁷, J. Khubua^{154b}, S. Kido⁸⁰, M. Kiehn³⁴, A. Kilgallon¹²⁶, E. Kim¹⁵⁹, Y. K. Kim³⁵, N. Kimura⁹², A. Kirchhoff⁵¹, D. Kirchmeier⁴⁶, C. Kirfel²², J. Kirk¹³⁸, A. E. Kiryunin¹¹¹, T. Kishimoto¹⁵⁸, D. P. Kisluk¹⁶¹, C. Kitsaki⁹, O. Kivernyk²², T. Klapdor-Kleingrothaus⁵⁰, M. Klassen^{59a}, C. Klein³², L. Klein¹⁷¹, M. H. Klein¹⁰², M. Klein⁸⁸, U. Klein⁸⁸, P. Klimek³⁴, A. Klimentov²⁷, F. Klimpel¹¹¹, T. Klingl²², T. Klioutchnikova³⁴, F. F. Klitzner¹¹⁰, P. Kluit¹¹⁵, S. Kluth¹¹¹, E. Kneringer⁷⁴, T. M. Knight¹⁶¹, A. Knue⁵⁰, D. Kobayashi⁸⁵, R. Kobayashi⁸³, M. Kobel⁴⁶, M. Kocian¹⁴⁸, T. Kodama¹⁵⁸, P. Kodys¹³⁷, D. M. Koeck¹⁵¹, P. T. Koenig²², T. Koffas³², N. M. Köhler³⁴, M. Kolb¹³⁹, I. Koletsou⁴, T. Komarek¹²⁵, K. Köneke⁵⁰, A. X. Y. Kong¹, T. Kono¹²¹, V. Konstantinides⁹², N. Konstantinidis⁹², B. Konya⁹⁴, R. Kopeliansky⁶³, S. Koperny^{81a}, K. Korcyl⁸², K. Kordas¹⁵⁷, G. Koren¹⁵⁶, A. Korn⁹², S. Korn⁵¹, I. Korolkov¹², E. V. Korolkova¹⁴⁴, N. Korotkova¹⁰⁹, B. Kortman¹¹⁵, O. Kortner¹¹¹, S. Kortner¹¹¹, W. H. Kostecka¹¹⁶, V. V. Kostyukhin^{146,160}, A. Kotsokechagia⁶², A. Kotwal⁴⁷, A. Koulouris³⁴, A. Kourkoumeli-Charalampidi^{68a,68b}, C. Kourkoumelis⁸,

E. Kourlitis⁵, O. Kovanda¹⁵¹, R. Kowalewski¹⁷⁰, W. Kozanecki¹³⁹, A. S. Kozhin¹¹⁸, V. A. Kramarenko¹⁰⁹, G. Kramberger⁸⁹, P. Kramer⁹⁶, D. Krasnopevtsev^{58a}, M. W. Krasny¹³⁰, A. Krasznahorkay³⁴, J. A. Kremer⁹⁶, J. Kretzschmar⁸⁸, K. Kreul¹⁷, P. Krieger¹⁶¹, F. Krieter¹¹⁰, S. Krishnamurthy⁹⁹, A. Krishnan^{59b}, M. Krivos¹³⁷, K. Krizka¹⁶, K. Kroeninger⁴⁵, H. Kroha¹¹¹, J. Kroll¹³⁵, J. Kroll¹³¹, K. S. Krowpman¹⁰³, U. Kruchonak⁷⁷, H. Krüger²², N. Krumnack⁷⁶, M. C. Kruse⁴⁷, J. A. Krzysiak⁸², A. Kubota¹⁵⁹, O. Kuchinskaia¹⁶⁰, S. Kuday^{3a}, D. Kuechler⁴⁴, J. T. Kuechler⁴⁴, S. Kuehn³⁴, T. Kuhl⁴⁴, V. Kukhtin⁷⁷, Y. Kulchitsky^{104.ad}, S. Kuleshov^{141d}, M. Kumar^{31g}, N. Kumari⁹⁸, M. Kuna⁵⁶, A. Kupco¹³⁵, T. Kupfer⁴⁵, O. Kuprash⁵⁰, H. Kurashige⁸⁰, L. L. Kurchaninov^{162a}, Y. A. Kurochkin¹⁰⁴, A. Kurova¹⁰⁸, M. G. Kurth^{13a,13d}, E. S. Kuwertz³⁴, M. Kuze¹⁵⁹, A. K. Kvam¹⁴³, J. Kvita¹²⁵, T. Kwan¹⁰⁰, K. W. Kwok^{60a}, C. Lacasta¹⁶⁸, F. Lacava^{70a,70b}, H. Lacker¹⁷, D. Lacour¹³⁰, N. N. Lad⁹², E. Ladygin⁷⁷, R. Lafaye⁴, B. Laforge¹³⁰, T. Lagouri^{141e}, S. Lai⁵¹, I. K. Lakomic^{81a}, N. Lalloue⁵⁶, J. E. Lambert¹²³, S. Lammers⁶³, W. Lampl¹⁶, C. Lampoudis¹⁵⁷, E. Lançon²⁷, U. Landgraf⁵⁰, M. P. J. Landon⁹⁰, V. S. Lang⁵⁰, J. C. Lange⁵¹, R. J. Langenberg⁹⁹, A. J. Lankford¹⁶⁵, F. Lanni²⁷, K. Lantzsch²², A. Lanza^{68a}, A. Lapertosa^{53a,53b}, J. F. Laporte¹³⁹, T. Lari^{66a}, F. Lasagni Manghi^{21b}, M. Lassnig³⁴, V. Latonova¹³⁵, T. S. Lau^{60a}, A. Laudrain⁹⁶, A. Laurier³², M. Lavorgna^{67a,67b}, S. D. Lawlor⁹¹, Z. Lawrence⁹⁷, M. Lazzaroni^{66a,66b}, B. Le⁹⁷, B. Leban⁸⁹, A. Lebedev⁷⁶, M. LeBlanc³⁴, T. LeCompte⁵, F. Ledroit-Guillon⁵⁶, A. C. A. Lee⁹², G. R. Lee¹⁵, L. Lee⁵⁷, S. C. Lee¹⁵³, S. Lee⁷⁶, L. L. Leeuw^{31c}, B. Lefebvre^{162a}, H. P. Lefebvre⁹¹, M. Lefebvre¹⁷⁰, C. Leggett¹⁶, K. Lehmann¹⁴⁷, N. Lehmann¹⁸, G. Lehmann Miotto³⁴, W. A. Leight⁴⁴, A. Leisos^{157.u}, M. A. L. Leite^{78c}, C. E. Leitgeb⁴⁴, R. Leitner¹³⁷, K. J. C. Leney⁴⁰, T. Lenz²², S. Leone^{69a}, C. Leonidopoulos⁴⁸, A. Leopold¹⁴⁹, C. Leroy¹⁰⁶, R. Les¹⁰³, C. G. Lester³⁰, M. Levchenko¹³², J. Levêque⁴, D. Levin¹⁰², L. J. Levinson¹⁷⁴, D. J. Lewis¹⁹, B. Li^{13b}, B. Li^{58b}, C. Li^{58a}, C.-Q. Li^{58c,58d}, H. Li^{58a}, H. Li^{58b}, H. Li^{58b}, J. Li^{58c}, K. Li¹⁴³, L. Li^{58c}, M. Li^{13a,13d}, Q. Y. Li^{58a}, S. Li^{58c,58d.c}, T. Li^{58b}, X. Li⁴⁴, Y. Li⁴⁴, Z. Li^{58b}, Z. Li¹²⁹, Z. Li¹⁰⁰, Z. Li⁸⁸, Z. Liang^{13a}, M. Liberatore⁴⁴, B. Liberti^{71a}, K. Lie^{60c}, J. Lieber Marin^{78b}, K. Lin¹⁰³, R. A. Linck⁶³, R. E. Lindley⁶, J. H. Lindon², A. Linss⁴⁴, E. Lipeles¹³¹, A. Lipniacka¹⁵, T. M. Liss^{167.ab}, A. Lister¹⁶⁹, J. D. Little⁷, B. Liu^{13a}, B. X. Liu¹⁴⁷, J. B. Liu^{58a}, J. K. K. Liu³⁵, K. Liu^{58c,58d}, M. Liu^{58a}, M. Y. Liu^{58a}, P. Liu^{13a}, Q. Liu^{58c,58d,144}, X. Liu^{58a}, Y. Liu⁴⁴, Y. Liu^{13c,13d}, Y. L. Liu¹⁰², Y. W. Liu^{58a}, M. Livan^{68a,68b}, J. Llorente Merino¹⁴⁷, S. L. Lloyd⁹⁰, E. M. Lobodzinska⁴⁴, P. Loch⁶, S. Loffredo^{71a,71b}, T. Lohse¹⁷, K. Lohwasser¹⁴⁴, M. Lokajicek¹³⁵, J. D. Long¹⁶⁷, I. Longarini^{70a,70b}, L. Longo³⁴, R. Longo¹⁶⁷, I. Lopez Paz¹², A. Lopez Solis⁴⁴, J. Lorenz¹¹⁰, N. Lorenzo Martinez⁴, A. M. Lory¹¹⁰, A. Lösle⁵⁰, X. Lou^{43a,43b}, X. Lou^{13a}, A. Lounis⁶², J. Love⁵, P. A. Love⁸⁷, J. J. Lozano Bahilo¹⁶⁸, G. Lu^{13a}, M. Lu^{58a}, S. Lu¹³¹, Y. J. Lu⁶¹, H. J. Lubatti¹⁴³, C. Luci^{70a,70b}, F. L. Lucio Alves^{13c}, A. Lucotte⁵⁶, F. Luehring⁶³, I. Luise¹⁵⁰, L. Luminari^{70a}, O. Lundberg¹⁴⁹, B. Lund-Jensen¹⁴⁹, N. A. Luongo¹²⁶, M. S. Lutz¹⁵⁶, D. Lynn²⁷, H. Lyons⁸⁸, R. Lysak¹³⁵, E. Lytken⁹⁴, F. Lyu^{13a}, V. Lyubushkin⁷⁷, T. Lyubushkina⁷⁷, H. Ma²⁷, L. L. Ma^{58b}, Y. Ma⁹², D. M. Mac Donell¹⁷⁰, G. Maccarrone⁴⁹, C. M. Macdonald¹⁴⁴, J. C. MacDonald¹⁴⁴, R. Madar³⁶, W. F. Mader⁴⁶, M. Madugoda Ralalage Don¹²⁴, N. Madysa⁴⁶, J. Maeda⁸⁰, T. Maeno²⁷, M. Maerker⁴⁶, V. Magerl⁵⁰, J. Magro^{64a,64c}, D. J. Mahon³⁷, C. Maidantchik^{78b}, A. Maio^{134a,134b,134d}, K. Maj^{81a}, O. Majersky^{26a}, S. Majewski¹²⁶, N. Makovec⁶², V. Maksimovic¹⁴, B. Malaescu¹³⁰, Pa. Malecki⁸², V. P. Maleev¹³², F. Malek⁵⁶, D. Malito^{39a,39b}, U. Mallik⁷⁵, C. Malone³⁰, S. Maltezos⁹, S. Malyukov⁷⁷, J. Mamuzic¹⁶⁸, G. Mancini⁴⁹, J. P. Mandalia⁹⁰, I. Mandić⁸⁹, L. Manhaes de Andrade Filho^{78a}, I. M. Maniatis¹⁵⁷, M. Manisha¹³⁹, J. Manjarres Ramos⁴⁶, K. H. Mankinen⁹⁴, A. Mann¹¹⁰, A. Manousos⁷⁴, B. Mansoulie¹³⁹, I. Manthos¹⁵⁷, S. Manzoni¹¹⁵, A. Marantis^{157.u}, G. Marchiori¹³⁰, M. Marcisovsky¹³⁵, L. Marcoccia^{71a,71b}, C. Marcon⁹⁴, M. Marjanovic¹²³, Z. Marshall¹⁶, S. Marti-Garcia¹⁶⁸, T. A. Martin¹⁷², V. J. Martin⁴⁸, B. Martin dit Latour¹⁵, L. Martinelli^{70a,70b}, M. Martinez^{12.v}, P. Martinez Agullo¹⁶⁸, V. I. Martinez Outschoorn⁹⁹, S. Martin-Haugh¹³⁸, V. S. Martoiu^{25b}, A. C. Martyniuk⁹², A. Marzin³⁴, S. R. Maschek¹¹¹, L. Masetti⁹⁶, T. Mashimo¹⁵⁸, J. Masik⁹⁷, A. L. Maslennikov^{117a,117b}, L. Massa^{21b}, P. Massarotti^{67a,67b}, P. Mastrandrea^{69a,69b}, A. Mastroberardino^{39a,39b}, T. Masubuchi¹⁵⁸, D. Matakias²⁷, T. Mathisen¹⁶⁶, A. Matic¹¹⁰, N. Matsuzawa¹⁵⁸, J. Maurer^{25b}, B. Maček⁸⁹, D. A. Maximov^{117a,117b}, R. Mazini¹⁵³, I. Maznas¹⁵⁷, S. M. Mazza¹⁴⁰, C. Mc Ginn²⁷, J. P. Mc Gowan¹⁰⁰, S. P. Mc Kee¹⁰², T. G. McCarthy¹¹¹, W. P. McCormack¹⁶, E. F. McDonald¹⁰¹, A. E. McDougall¹¹⁵, J. A. Mcfayden¹⁵¹, G. Mchedlidge^{154b}, M. A. McKay⁴⁰, K. D. McLean¹⁷⁰, S. J. McMahan¹³⁸, P. C. McNamara¹⁰¹, R. A. McPherson^{170.y}, J. E. Mdhului^{31g}, Z. A. Meadows⁹⁹, S. Meehan³⁴, T. Megy³⁶, S. Mehlhase¹¹⁰, A. Mehta⁸⁸, B. Meirose⁴¹, D. Melini¹⁵⁵, B. R. Mellado Garcia^{31g}, A. H. Melo⁵¹, F. Meloni⁴⁴, A. Melzer²², E. D. Mendes Gouveia^{134a}, A. M. Mendes Jacques Da Costa¹⁹, H. Y. Meng¹⁶¹, L. Meng³⁴, S. Menke¹¹¹

M. Mentink³⁴, E. Meoni^{39a,39b}, C. Merlassino¹²⁹, P. Mermod^{52,*}, L. Merola^{67a,67b}, C. Meroni^{66a}, G. Merz¹⁰², O. Meshkov^{107,109}, J. K. R. Meshreki¹⁴⁶, J. Metcalfe⁵, A. S. Mete⁵, C. Meyer⁶³, J.-P. Meyer¹³⁹, M. Michetti¹⁷, R. P. Middleton¹³⁸, L. Mijović⁴⁸, G. Mikenberg¹⁷⁴, M. Mikestikova¹³⁵, M. Mikuz⁸⁹, H. Mildner¹⁴⁴, A. Milic¹⁶¹, C. D. Milke⁴⁰, D. W. Miller³⁵, L. S. Miller³², A. Milov¹⁷⁴, D. A. Milstead^{43a,43b}, T. Min^{13c}, A. A. Minaenko¹¹⁸, I. A. Minashvili^{154b}, L. Mince⁵⁵, A. I. Mincer¹²⁰, B. Mindur^{81a}, M. Mineev⁷⁷, Y. Minegishi¹⁵⁸, Y. Mino⁸³, L. M. Mir¹², M. Miralles Lopez¹⁶⁸, M. Mironova¹²⁹, T. Mitani¹⁷³, V. A. Mitsou¹⁶⁸, M. Mittal^{58c}, O. Miu¹⁶¹, P. S. Miyagawa⁹⁰, Y. Miyazaki⁸⁵, A. Mizukami⁷⁹, J. U. Mjörnmark⁹⁴, T. Mkrtchyan^{59a}, M. Mlynarikova¹¹⁶, T. Moa^{43a,43b}, S. Mobius⁵¹, K. Mochizuki¹⁰⁶, P. Moder⁴⁴, P. Mogg¹¹⁰, A. F. Mohammed^{13a}, S. Mohapatra³⁷, G. Mokgatitswane^{31g}, B. Mondal¹⁴⁶, S. Mondal¹³⁶, K. Mönig⁴⁴, E. Monnier⁹⁸, L. Monsonis Romero¹⁶⁸, A. Montalbano¹⁴⁷, J. Montejo Berlingen³⁴, M. Montella¹²², F. Monticelli⁸⁶, N. Morange⁶², A. L. Moreira De Carvalho^{134a}, M. Moreno Llácer¹⁶⁸, C. Moreno Martinez¹², P. Moretini^{53b}, S. Morgenstern¹⁷², D. Mori¹⁴⁷, M. Morii⁵⁷, M. Morinaga¹⁵⁸, V. Morisbak¹²⁸, A. K. Morley³⁴, A. P. Morris⁹², L. Morvaj³⁴, P. Moschovakos³⁴, B. Moser¹¹⁵, M. Mosidze^{154b}, T. Moskalets⁵⁰, P. Moskvitina¹¹⁴, J. Moss^{29,n}, E. J. W. Moyses⁹⁹, S. Muanza⁹⁸, J. Mueller¹³³, R. Mueller¹⁸, D. Muenstermann⁸⁷, G. A. Mullier⁹⁴, J. J. Mullin¹³¹, D. P. Mungo^{66a,66b}, J. L. Munoz Martinez¹², F. J. Munoz Sanchez⁹⁷, M. Murin⁹⁷, P. Murin^{26b}, W. J. Murray^{138,172}, A. Murrone^{66a,66b}, J. M. Muse¹²³, M. Muškinja¹⁶, C. Mwewa²⁷, A. G. Myagkov^{118,ac}, A. J. Myers⁷, A. A. Myers¹³³, G. Myers⁶³, M. Myska¹³⁶, B. P. Nachman¹⁶, O. Nackenhorst⁴⁵, A. Nag Nag⁴⁶, K. Nagai¹²⁹, K. Nagano⁷⁹, J. L. Nagle²⁷, E. Nagy⁹⁸, A. M. Nairz³⁴, Y. Nakahama¹¹², K. Nakamura⁷⁹, H. Nanjo¹²⁷, F. Napolitano^{59a}, R. Narayan⁴⁰, E. A. Narayanan¹¹³, I. Naryshkin¹³², M. Naseri³², C. Nass²², T. Naumann⁴⁴, G. Navarro^{20a}, J. Navarro-Gonzalez¹⁶⁸, R. Nayak¹⁵⁶, P. Y. Nechaeva¹⁰⁷, F. Nechansky⁴⁴, T. J. Neep¹⁹, A. Negri^{68a,68b}, M. Negrini^{21b}, C. Nellist¹¹⁴, C. Nelson¹⁰⁰, K. Nelson¹⁰², S. Nemecek¹³⁵, M. Nessi^{34,f}, M. S. Neubauer¹⁶⁷, F. Neuhaus⁹⁶, J. Neundorff⁴⁴, R. Newhouse¹⁶⁹, P. R. Newman¹⁹, C. W. Ng¹³³, Y. S. Ng¹⁷, Y. W. Y. Ng¹⁶⁵, B. Ngair^{33e}, H. D. N. Nguyen¹⁰⁶, R. B. Nickerson¹²⁹, R. Nicolaidou¹³⁹, D. S. Nielsen³⁸, J. Nielsen¹⁴⁰, M. Niemeyer⁵¹, N. Nikiforou¹⁰, V. Nikolaenko^{118,ae}, I. Nikolic-Audit¹³⁰, K. Nikolopoulos¹⁹, P. Nilsson²⁷, H. R. Nindhito⁵², A. Nisati^{70a}, N. Nishu², R. Nisius¹¹¹, T. Nitta¹⁷³, T. Nobe¹⁵⁸, D. L. Noel³⁰, Y. Noguchi⁸³, I. Nomidis¹³⁰, M. A. Nomura²⁷, M. B. Norfolk¹⁴⁴, R. R. B. Norisam⁹², J. Novak⁸⁹, T. Novak⁴⁴, O. Novgorodova⁴⁶, L. Novotny¹³⁶, R. Novotny¹¹³, L. Nozka¹²⁵, K. Ntekas¹⁶⁵, E. Nurse⁹², F. G. Oakham^{32,ai}, J. Ocariz¹³⁰, A. Ochi⁸⁰, I. Ochoa^{134a}, J. P. Ochoa-Ricoux^{141a}, S. Oda⁸⁵, S. Odaka⁷⁹, S. Oerdek¹⁶⁶, A. Ogrodnik^{81a}, A. Oh⁹⁷, C. C. Ohm¹⁴⁹, H. Oide¹⁵⁹, R. Oishi¹⁵⁸, M. L. Ojeda⁴⁴, Y. Okazaki⁸³, M. W. O'Keefe⁸⁸, Y. Okumura¹⁵⁸, A. Olariu^{25b}, L. F. Oleiro Seabra^{134a}, S. A. Olivares Pino^{141e}, D. Oliveira Damazio²⁷, D. Oliveira Goncalves^{78a}, J. L. Oliver¹⁶⁵, M. J. R. Olsson¹⁶⁵, A. Olszewski⁸², J. Olszowska⁸², Ö. O. Öncel²², D. C. O'Neil¹⁴⁷, A. P. O'Neill¹²⁹, A. Onofre^{134a,134e}, P. U. E. Onyisi¹⁰, R. G. Oreamuno Madriz¹¹⁶, M. J. Oreglia³⁵, G. E. Orellana⁸⁶, D. Orestano^{72a,72b}, N. Orlando¹², R. S. Orr¹⁶¹, V. O'Shea⁵⁵, R. Ospanov^{58a}, G. Otero y Garzon²⁸, H. Otono⁸⁵, P. S. Ott^{59a}, G. J. Ottino¹⁶, M. Ouchrif^{33d}, J. Ouellette²⁷, F. Ould-Saada¹²⁸, A. Ourau^{139,*}, Q. Ouyang^{13a}, M. Owen⁵⁵, R. E. Owen¹³⁸, K. Y. Oyulmaz^{11c}, V. E. Ozcan^{11c}, N. Ozturk⁷, S. Ozturk^{11c}, J. Pacalt¹²⁵, H. A. Pacey³⁰, K. Pachal⁴⁷, A. Pacheco Pages¹², C. Padilla Aranda¹², S. Pagan Griso¹⁶, G. Palacino⁶³, S. Palazzo⁴⁸, S. Palestini³⁴, M. Palka^{81b}, P. Palni^{81a}, D. K. Panchal¹⁰, C. E. Pandini⁵², J. G. Panduro Vazquez⁹¹, P. Pani⁴⁴, G. Panizzo^{64a,64c}, L. Paolozzi⁵², C. Papadatos¹⁰⁶, S. Parajuli⁴⁰, A. Paramonov⁵, C. Paraskevopoulos⁹, D. Paredes Hernandez^{60b}, S. R. Paredes Saenz¹²⁹, B. Parida¹⁷⁴, T. H. Park¹⁶¹, A. J. Parker²⁹, M. A. Parker³⁰, F. Parodi^{53a,53b}, E. W. Parrish¹¹⁶, J. A. Parsons³⁷, U. Parzefall⁵⁰, L. Pascual Dominguez¹⁵⁶, V. R. Pascuzzi¹⁶, F. Pasquali¹¹⁵, E. Pasqualucci^{70a}, S. Passaggio^{53b}, F. Pastore⁹¹, P. Pasuan^{43a,43b}, J. R. Pater⁹⁷, A. Pathak¹⁷⁵, J. Patton⁸⁸, T. Pauly³⁴, J. Parkes¹⁴⁸, M. Pedersen¹²⁸, L. Pedraza Diaz¹¹⁴, R. Pedro^{134a}, T. Peiffer⁵¹, S. V. Peleganchuk^{117a,117b}, O. Penc¹³⁵, C. Peng^{60b}, H. Peng^{58a}, M. Penzin¹⁶⁰, B. S. Peralva^{78a}, A. P. Pereira Peixoto^{134a}, L. Pereira Sanchez^{43a,43b}, D. V. Perepelitsa²⁷, E. Perez Codina^{162a}, M. Perganti⁹, L. Perini^{66a,66b}, H. Pernegger³⁴, S. Perrella³⁴, A. Perrevoort¹¹⁵, K. Peters⁴⁴, R. F. Y. Peters⁹⁷, B. A. Petersen³⁴, T. C. Petersen³⁸, E. Petit⁹⁸, V. Petousis¹³⁶, C. Petridou¹⁵⁷, P. Petroff⁶², F. Petrucci^{72a,72b}, A. Petrukhin¹⁴⁶, M. Pettee¹⁷⁷, N. E. Pettersson³⁴, K. Petukhova¹³⁷, A. Peyaud¹³⁹, R. Pezoa^{141f}, L. Pezzotti³⁴, G. Pezzullo¹⁷⁷, T. Pham¹⁰¹, P. W. Phillips¹³⁸, M. W. Phipps¹⁶⁷, G. Piacquadio¹⁵⁰, E. Pianori¹⁶, F. Piazza^{66a,66b}, A. Picazio⁹⁹, R. Piegaia²⁸, D. Pietreanu^{25b}, J. E. Pilcher³⁵, A. D. Pilkington⁹⁷, M. Pinamonti^{64a,64c}, J. L. Pinfold², C. Pitman Donaldson⁹², D. A. Pizzi³², L. Pizzimento^{71a,71b}, A. Pizzini¹¹⁵, M.-A. Pleier²⁷, V. Plesanovs⁵⁰,

S. Simion⁶², R. Simoniello³⁴, N. D. Simpson⁹⁴, S. Simsek^{11b}, P. Sinervo¹⁶¹, V. Sinetkii¹⁰⁹, S. Singh¹⁴⁷, S. Singh¹⁶¹, S. Sinha⁴⁴, S. Sinha^{31g}, M. Sioli^{21a,21b}, I. Siral¹²⁶, S. Yu. Sivoklokov¹⁰⁹, J. Sjölin^{43a,43b}, A. Skaf⁵¹, E. Skorda⁹⁴, P. Skubic¹²³, M. Slawinska⁸², K. Sliwa¹⁶⁴, V. Smakhtin¹⁷⁴, B. H. Smart¹³⁸, J. Smiesko¹³⁷, S. Yu. Smirnov¹⁰⁸, Y. Smirnov¹⁰⁸, L. N. Smirnova^{109,r}, O. Smirnova⁹⁴, E. A. Smith³⁵, H. A. Smith¹²⁹, M. Smizanska⁸⁷, K. Smolek¹³⁶, A. Smykiewicz⁸², A. A. Snesarev¹⁰⁷, H. L. Snoek¹¹⁵, S. Snyder²⁷, R. Sobie^{170,y}, A. Soffer¹⁵⁶, F. Sohns⁵¹, C. A. Solans Sanchez³⁴, E. Yu. Soldatov¹⁰⁸, U. Soldevila¹⁶⁸, A. A. Solodkov¹¹⁸, S. Solomon⁵⁰, A. Soloshenko⁷⁷, O. V. Solovyanov¹¹⁸, V. Solovye¹³², P. Sommer¹⁴⁴, H. Son¹⁶⁴, A. Sonay¹², W. Y. Song^{162b}, A. Sopczak¹³⁶, A. L. Sopio⁹², F. Sopkova^{26b}, S. Sottocornola^{68a,68b}, R. Soualah^{64a,64c}, A. M. Soukharev^{117a,117b}, Z. Soumami^{33e}, D. South⁴⁴, S. Spagnolo^{65a,65b}, M. Spalla¹¹¹, M. Spangenberg¹⁷², F. Spanò⁹¹, D. Sperlich⁵⁰, T. M. Spieker^{59a}, G. Spigo³⁴, M. Spina¹⁵¹, D. P. Spiteri⁵⁵, M. Spousta¹³⁷, A. Stabile^{66a,66b}, B. L. Stamas¹¹⁶, R. Stamen^{59a}, M. Stamenkovic¹¹⁵, A. Stampekis¹⁹, M. Standke²², E. Stanecka⁸², B. Stanislaus³⁴, M. M. Stanitzki⁴⁴, M. Stankaityte¹²⁹, B. Stapf⁴⁴, E. A. Starchenko¹¹⁸, G. H. Stark¹⁴⁰, J. Stark⁹⁸, D. M. Starko^{162b}, P. Staroba¹³⁵, P. Starovoitov^{59a}, S. Stärz¹⁰⁰, R. Staszewski⁸², G. Stavropoulos⁴², P. Steinberg²⁷, A. L. Steinhebel¹²⁶, B. Stelzer^{147,162a}, H. J. Stelzer¹³³, O. Stelzer-Chilton^{162a}, H. Stenzel⁵⁴, T. J. Stevenson¹⁵¹, G. A. Stewart³⁴, M. C. Stockton³⁴, G. Stoicea^{25b}, M. Stolarski^{134a}, S. Stonjek¹¹¹, A. Straessner⁴⁶, J. Strandberg¹⁴⁹, S. Strandberg^{43a,43b}, M. Strauss¹²³, T. Strebler⁹⁸, P. Strizenec^{26b}, R. Ströhmer¹⁷¹, D. M. Strom¹²⁶, L. R. Strom⁴⁴, R. Stroynowski⁴⁰, A. Strubig^{43a,43b}, S. A. Stucci²⁷, B. Stugu¹⁵, J. Stupak¹²³, N. A. Styles⁴⁴, D. Su¹⁴⁸, S. Su^{58a}, W. Su^{58c,58d,144}, X. Su^{58a}, K. Sugizaki¹⁵⁸, V. V. Sulin¹⁰⁷, M. J. Sullivan⁸⁸, D. M. S. Sultan⁵², L. Sultanaliyeva¹⁰⁷, S. Sultansoy^{3c}, T. Sumida⁸³, S. Sun¹⁰², S. Sun¹⁷⁵, X. Sun⁹⁷, O. Sunneborn Gudnadottir¹⁶⁶, C. J. E. Suster¹⁵², M. R. Sutton¹⁵¹, M. Svatos¹³⁵, M. Swiatlowski^{162a}, T. Swirski¹⁷¹, I. Sykora^{26a}, M. Sykora¹³⁷, T. Sykora¹³⁷, D. Ta⁹⁶, K. Tackmann^{44,w}, A. Taffard¹⁶⁵, R. Tafirout^{162a}, R. H. M. Taibah¹³⁰, R. Takashima⁸⁴, K. Takeda⁸⁰, T. Takeshita¹⁴⁵, E. P. Takeva⁴⁸, Y. Takubo⁷⁹, M. Talby⁹⁸, A. A. Talyshev^{117a,117b}, K. C. Tam^{60b}, N. M. Tamir¹⁵⁶, A. Tanaka¹⁵⁸, J. Tanaka¹⁵⁸, R. Tanaka⁶², J. Tang^{58c}, Z. Tao¹⁶⁹, S. Tapia Araya⁷⁶, S. Tapprogge⁹⁶, A. Tarek Abouelfadl Mohamed¹⁰³, S. Tarem¹⁵⁵, K. Tariq^{58b}, G. Tarna^{25b}, G. F. Tartarelli^{66a}, P. Tas¹³⁷, M. Tasevsky¹³⁵, E. Tassi^{39a,39b}, G. Tateno¹⁵⁸, Y. Tayalati^{33e}, G. N. Taylor¹⁰¹, W. Taylor^{162b}, H. Teagle⁸⁸, A. S. Tee¹⁷⁵, R. Teixeira De Lima¹⁴⁸, P. Teixeira-Dias⁹¹, H. Ten Kate³⁴, J. J. Teoh¹¹⁵, K. Terashi¹⁵⁸, J. Terron⁹⁵, S. Terzo¹², M. Testa⁴⁹, R. J. Teuscher^{161,y}, N. Themistokleous⁴⁸, T. Thevenaux-Pelzer¹⁷, O. Thielmann¹⁷⁶, D. W. Thomas⁹¹, J. P. Thomas¹⁹, E. A. Thompson⁴⁴, P. D. Thompson¹⁹, E. Thomson¹³¹, E. J. Thorpe⁹⁰, Y. Tian⁵¹, V. O. Tikhomirov^{107,af}, Yu. A. Tikhonov^{117a,117b}, S. Timoshenko¹⁰⁸, P. Tipton¹⁷⁷, S. Tisserant⁹⁸, S. H. Tlou^{31g}, A. Tmourji³⁶, K. Todome^{21a,21b}, S. Todorova-Nova¹³⁷, S. Todt⁴⁶, M. Togawa⁷⁹, J. Tojo⁸⁵, S. Tokár^{26a}, K. Tokushuku⁷⁹, E. Tolley¹²², R. Tombs³⁰, M. Tomoto^{79,112}, L. Tompkins¹⁴⁸, P. Tornambe⁹⁹, E. Torrence¹²⁶, H. Torres⁴⁶, E. Torró Pastor¹⁶⁸, M. Toscani²⁸, C. Tosciri³⁵, J. Toth^{98,x}, D. R. Tovey¹⁴⁴, A. Traeet¹⁵, C. J. Treado¹²⁰, T. Trefzger¹⁷¹, A. Tricoli²⁷, I. M. Trigger^{162a}, S. Trincaz-Duvoid¹³⁰, D. A. Trischuk¹⁶⁹, W. Trischuk¹⁶¹, B. Trocmé⁵⁶, A. Trofymov⁶², C. Troncon^{66a}, F. Trovato¹⁵¹, L. Truong^{31c}, M. Trzebinski⁸², A. Trzupek⁸², F. Tsai¹⁵⁰, M. Tsai¹⁰², A. Tsiamis¹⁵⁷, P. V. Tsiarshka¹⁰⁴, A. Tsigotis^{157,u}, V. Tsiskaridze¹⁵⁰, E. G. Tskhadadze^{154a}, M. Tsopoulou¹⁵⁷, Y. Tsujikawa⁸³, I. I. Tsukerman¹¹⁹, V. Tsulaia¹⁶, S. Tsuno⁷⁹, O. Tsur¹⁵⁵, D. Tsybychev¹⁵⁰, Y. Tu^{60b}, A. Tudorache^{25b}, V. Tudorache^{25b}, A. N. Tuna³⁴, S. Turchikhin⁷⁷, I. Turk Cakir^{3a}, R. J. Turner¹⁹, R. Turra^{66a}, P. M. Tuts³⁷, S. Tzamarias¹⁵⁷, P. Tzanis⁹, E. Tzovara⁹⁶, K. Uchida¹⁵⁸, F. Ukegawa¹⁶³, P. A. Ulloa Poblete^{141c}, G. Unal³⁴, M. Unal¹⁰, A. Undrus²⁷, G. Unel¹⁶⁵, F. C. Ungaro¹⁰¹, K. Uno¹⁵⁸, J. Urban^{26b}, P. Urquijo¹⁰¹, G. Usai⁷, R. Ushioda¹⁵⁹, M. Usman¹⁰⁶, Z. Uysal^{11d}, V. Vacek¹³⁶, B. Vachon¹⁰⁰, K. O. H. Vadla¹²⁸, T. Vafeiadis³⁴, C. Valderanis¹¹⁰, E. Valdes Santurio^{43a,43b}, M. Valente^{162a}, S. Valentineti^{21a,21b}, A. Valero¹⁶⁸, R. A. Vallance¹⁹, A. Vallier⁹⁸, J. A. Valls Ferrer¹⁶⁸, T. R. Van Daalen¹⁴³, P. Van Gemmeren⁵, S. Van Stroud⁹², I. Van Vulpen¹¹⁵, M. Vanadia^{71a,71b}, W. Vandelli³⁴, M. Vandenbroucke¹³⁹, E. R. Vandewall¹²⁴, D. Vannicola¹⁵⁶, L. Vannoli^{53a,53b}, R. Vari^{70a}, E. W. Varnes⁶, C. Varni¹⁶, T. Varol¹⁵³, D. Varouchas⁶², K. E. Varvell¹⁵², M. E. Vasile^{25b}, L. Vaslin³⁶, G. A. Vasquez¹⁷⁰, F. Vazeille³⁶, D. Vazquez Furelos¹², T. Vazquez Schroeder³⁴, J. Veatch⁵¹, V. Vecchio⁹⁷, M. J. Veer¹¹⁵, I. Veliscek¹²⁹, L. M. Veloce¹⁶¹, F. Veloso^{134a,134c}, S. Veneziano^{70a}, A. Ventura^{65a,65b}, A. Verbytskyi¹¹¹, M. Verducci^{69a,69b}, C. Vergis²², M. Verissimo De Araujo^{78b}, W. Verkerke¹¹⁵, A. T. Vermeulen¹¹⁵, J. C. Vermeulen¹¹⁵, C. Vernieri¹⁴⁸, P. J. Verschuur⁹¹, M. Vessella⁹⁹, M. L. Vesterbacka¹²⁰, M. C. Vetterli^{147,ai}, A. Vgenopoulos¹⁵⁷, N. Viaux Maira^{141f}, T. Vickey¹⁴⁴, O. E. Vickey Boeriu¹⁴⁴, G. H. A. Viehhauser¹²⁹, L. Vighi^{59b}, M. Villa^{21a,21b}, M. Villaplana Perez¹⁶⁸

- ¹³ (a)Institute of High Energy Physics, Chinese Academy of Sciences, Beijing, China; (b)Physics Department, Tsinghua University, Beijing, China; (c)Department of Physics, Nanjing University, Nanjing, China; (d)University of Chinese Academy of Science (UCAS), Beijing, China
- ¹⁴ Institute of Physics, University of Belgrade, Belgrade, Serbia
- ¹⁵ Department for Physics and Technology, University of Bergen, Bergen, Norway
- ¹⁶ Physics Division, Lawrence Berkeley National Laboratory and University of California, Berkeley, CA, USA
- ¹⁷ Institut für Physik, Humboldt Universität zu Berlin, Berlin, Germany
- ¹⁸ Albert Einstein Center for Fundamental Physics and Laboratory for High Energy Physics, University of Bern, Bern, Switzerland
- ¹⁹ School of Physics and Astronomy, University of Birmingham, Birmingham, UK
- ²⁰ (a)Facultad de Ciencias y Centro de Investigaciones, Universidad Antonio Nariño, Bogotá, Colombia; (b)Departamento de Física, Universidad Nacional de Colombia, Bogotá, Colombia
- ²¹ (a)Dipartimento di Fisica e Astronomia A. Righi, Università di Bologna, Bologna, Italy; (b)INFN Sezione di Bologna, Bologna, Italy
- ²² Physikalisches Institut, Universität Bonn, Bonn, Germany
- ²³ Department of Physics, Boston University, Boston, MA, USA
- ²⁴ Department of Physics, Brandeis University, Waltham, MA, USA
- ²⁵ (a)Transilvania University of Brasov, Brasov, Romania; (b)Horia Hulubei National Institute of Physics and Nuclear Engineering, Bucharest, Romania; (c)Department of Physics, Alexandru Ioan Cuza University of Iasi, Iasi, Romania; (d)Physics Department, National Institute for Research and Development of Isotopic and Molecular Technologies, Cluj-Napoca, Romania; (e)University Politehnica Bucharest, Bucharest, Romania; (f)West University in Timisoara, Timisoara, Romania
- ²⁶ (a)Faculty of Mathematics, Physics and Informatics, Comenius University, Bratislava, Slovak Republic; (b)Department of Subnuclear Physics, Institute of Experimental Physics of the Slovak Academy of Sciences, Kosice, Slovak Republic
- ²⁷ Physics Department, Brookhaven National Laboratory, Upton, NY, USA
- ²⁸ Departamento de Física (FCEN) and IFIBA, Universidad de Buenos Aires and CONICET, Buenos Aires, Argentina
- ²⁹ California State University, Long Beach, CA, USA
- ³⁰ Cavendish Laboratory, University of Cambridge, Cambridge, UK
- ³¹ (a)Department of Physics, University of Cape Town, Cape Town, South Africa; (b)iThemba Labs, Cape Town, Western Cape, South Africa; (c)Department of Mechanical Engineering Science, University of Johannesburg, Johannesburg, South Africa; (d)National Institute of Physics, University of the Philippines Diliman, Quezon City, Philippines; (e)University of South Africa, Department of Physics, Pretoria, South Africa; (f)University of Zululand, KwaDlangezwa, South Africa; (g)School of Physics, University of the Witwatersrand, Johannesburg, South Africa
- ³² Department of Physics, Carleton University, Ottawa, ON, Canada
- ³³ (a)Faculté des Sciences Ain Chock, Réseau Universitaire de Physique des Hautes Energies-Université Hassan II, Casablanca, Morocco; (b)Faculté des Sciences, Université Ibn-Tofail, Kenitra, Morocco; (c)Faculté des Sciences Semlalia, Université Cadi Ayyad, LPHEA-Marrakech, Marrakech, Morocco; (d)LPMR, Faculté des Sciences, Université Mohamed Premier, Oujda, Morocco; (e)Faculté des Sciences, Université Mohammed V, Rabat, Morocco; (f)Mohammed VI Polytechnic University, Ben Guerir, Morocco
- ³⁴ CERN, Geneva, Switzerland
- ³⁵ Enrico Fermi Institute, University of Chicago, Chicago, IL, USA
- ³⁶ LPC, Université Clermont Auvergne, CNRS/IN2P3, Clermont-Ferrand, France
- ³⁷ Nevis Laboratory, Columbia University, Irvington, NY, USA
- ³⁸ Niels Bohr Institute, University of Copenhagen, Copenhagen, Denmark
- ³⁹ (a)Dipartimento di Fisica, Università della Calabria, Rende, Italy; (b)INFN Gruppo Collegato di Cosenza, Laboratori Nazionali di Frascati, Frascati, Italy
- ⁴⁰ Physics Department, Southern Methodist University, Dallas, TX, USA
- ⁴¹ Physics Department, University of Texas at Dallas, Richardson, TX, USA
- ⁴² National Centre for Scientific Research “Demokritos”, Agia Paraskevi, Greece
- ⁴³ (a)Department of Physics, Stockholm University, Stockholm, Sweden; (b)Oskar Klein Centre, Stockholm, Sweden
- ⁴⁴ Deutsches Elektronen-Synchrotron DESY, Hamburg and Zeuthen, Germany
- ⁴⁵ Lehrstuhl für Experimentelle Physik IV, Technische Universität Dortmund, Dortmund, Germany
- ⁴⁶ Institut für Kern- und Teilchenphysik, Technische Universität Dresden, Dresden, Germany

- ⁴⁷ Department of Physics, Duke University, Durham, NC, USA
- ⁴⁸ SUPA-School of Physics and Astronomy, University of Edinburgh, Edinburgh, UK
- ⁴⁹ INFN e Laboratori Nazionali di Frascati, Frascati, Italy
- ⁵⁰ Physikalisches Institut, Albert-Ludwigs-Universität Freiburg, Freiburg, Germany
- ⁵¹ II. Physikalisches Institut, Georg-August-Universität Göttingen, Göttingen, Germany
- ⁵² Département de Physique Nucléaire et Corpusculaire, Université de Genève, Geneva, Switzerland
- ⁵³ ^(a)Dipartimento di Fisica, Università di Genova, Genoa, Italy; ^(b)INFN Sezione di Genova, Genoa, Italy
- ⁵⁴ II. Physikalisches Institut, Justus-Liebig-Universität Giessen, Giessen, Germany
- ⁵⁵ SUPA-School of Physics and Astronomy, University of Glasgow, Glasgow, UK
- ⁵⁶ LPSC, Université Grenoble Alpes, CNRS/IN2P3, Grenoble INP, Grenoble, France
- ⁵⁷ Laboratory for Particle Physics and Cosmology, Harvard University, Cambridge, MA, USA
- ⁵⁸ ^(a)Department of Modern Physics and State Key Laboratory of Particle Detection and Electronics, University of Science and Technology of China, Hefei, China; ^(b)Institute of Frontier and Interdisciplinary Science and Key Laboratory of Particle Physics and Particle Irradiation (MOE), Shandong University, Qingdao, China; ^(c)Key Laboratory for Particle Astrophysics and Cosmology (MOE), SKLPPC, School of Physics and Astronomy, Shanghai Jiao Tong University, Shanghai, China; ^(d)Tsung-Dao Lee Institute, Shanghai, China
- ⁵⁹ ^(a)Kirchhoff-Institut für Physik, Ruprecht-Karls-Universität Heidelberg, Heidelberg, Germany; ^(b)Physikalisches Institut, Ruprecht-Karls-Universität Heidelberg, Heidelberg, Germany
- ⁶⁰ ^(a)Department of Physics, Chinese University of Hong Kong, Shatin, N.T., Hong Kong, China; ^(b)Department of Physics, University of Hong Kong, Hong Kong, China; ^(c)Department of Physics and Institute for Advanced Study, Hong Kong University of Science and Technology, Clear Water Bay, Kowloon, Hong Kong, China
- ⁶¹ Department of Physics, National Tsing Hua University, Hsinchu, Taiwan
- ⁶² IJCLab, Université Paris-Saclay, CNRS/IN2P3, 91405 Orsay, France
- ⁶³ Department of Physics, Indiana University, Bloomington, IN, USA
- ⁶⁴ ^(a)INFN Gruppo Collegato di Udine, Sezione di Trieste, Udine, Italy; ^(b)ICTP, Trieste, Italy; ^(c)Dipartimento Politecnico di Ingegneria e Architettura, Università di Udine, Udine, Italy
- ⁶⁵ ^(a)INFN Sezione di Lecce, Lecce, Italy; ^(b)Dipartimento di Matematica e Fisica, Università del Salento, Lecce, Italy
- ⁶⁶ ^(a)INFN Sezione di Milano, Milan, Italy; ^(b)Dipartimento di Fisica, Università di Milano, Milan, Italy
- ⁶⁷ ^(a)INFN Sezione di Napoli, Naples, Italy; ^(b)Dipartimento di Fisica, Università di Napoli, Naples, Italy
- ⁶⁸ ^(a)INFN Sezione di Pavia, Pavia, Italy; ^(b)Dipartimento di Fisica, Università di Pavia, Pavia, Italy
- ⁶⁹ ^(a)INFN Sezione di Pisa, Pisa, Italy; ^(b)Dipartimento di Fisica E. Fermi, Università di Pisa, Pisa, Italy
- ⁷⁰ ^(a)INFN Sezione di Roma, Rome, Italy; ^(b)Dipartimento di Fisica, Sapienza Università di Roma, Rome, Italy
- ⁷¹ ^(a)INFN Sezione di Roma Tor Vergata, Rome, Italy; ^(b)Dipartimento di Fisica, Università di Roma Tor Vergata, Rome, Italy
- ⁷² ^(a)INFN Sezione di Roma Tre, Rome, Italy; ^(b)Dipartimento di Matematica e Fisica, Università Roma Tre, Rome, Italy
- ⁷³ ^(a)INFN-TIFPA, Povo, Italy; ^(b)Università degli Studi di Trento, Trento, Italy
- ⁷⁴ Institut für Astro- und Teilchenphysik, Leopold-Franzens-Universität, Innsbruck, Austria
- ⁷⁵ University of Iowa, Iowa City, IA, USA
- ⁷⁶ Department of Physics and Astronomy, Iowa State University, Ames, IA, USA
- ⁷⁷ Joint Institute for Nuclear Research, Dubna, Russia
- ⁷⁸ ^(a)Departamento de Engenharia Elétrica, Universidade Federal de Juiz de Fora (UFJF), Juiz de Fora, Brazil ; ^(b)Universidade Federal do Rio De Janeiro COPPE/EE/IF, Rio de Janeiro, Brazil; ^(c)Instituto de Física, Universidade de São Paulo, São Paulo, Brazil; ^(d)Rio de Janeiro State University, Rio de Janeiro, Brazil
- ⁷⁹ KEK, High Energy Accelerator Research Organization, Tsukuba, Japan
- ⁸⁰ Graduate School of Science, Kobe University, Kobe, Japan
- ⁸¹ ^(a)Faculty of Physics and Applied Computer Science, AGH University of Science and Technology, Kraków, Poland ; ^(b)Marian Smoluchowski Institute of Physics, Jagiellonian University, Kraków, Poland
- ⁸² Institute of Nuclear Physics Polish Academy of Sciences, Kraków, Poland
- ⁸³ Faculty of Science, Kyoto University, Kyoto, Japan
- ⁸⁴ Kyoto University of Education, Kyoto, Japan
- ⁸⁵ Research Center for Advanced Particle Physics and Department of Physics, Kyushu University, Fukuoka, Japan
- ⁸⁶ Instituto de Física La Plata, Universidad Nacional de La Plata and CONICET, La Plata, Argentina
- ⁸⁷ Physics Department, Lancaster University, Lancaster, UK

- ⁸⁸ Oliver Lodge Laboratory, University of Liverpool, Liverpool, UK
- ⁸⁹ Department of Experimental Particle Physics, Jožef Stefan Institute and Department of Physics, University of Ljubljana, Ljubljana, Slovenia
- ⁹⁰ School of Physics and Astronomy, Queen Mary University of London, London, UK
- ⁹¹ Department of Physics, Royal Holloway University of London, Egham, UK
- ⁹² Department of Physics and Astronomy, University College London, London, UK
- ⁹³ Louisiana Tech University, Ruston, LA, USA
- ⁹⁴ Fysiska institutionen, Lunds universitet, Lund, Sweden
- ⁹⁵ Departamento de Física Teórica C-15 and CIAFF, Universidad Autónoma de Madrid, Madrid, Spain
- ⁹⁶ Institut für Physik, Universität Mainz, Mainz, Germany
- ⁹⁷ School of Physics and Astronomy, University of Manchester, Manchester, UK
- ⁹⁸ CPPM, Aix-Marseille Université, CNRS/IN2P3, Marseille, France
- ⁹⁹ Department of Physics, University of Massachusetts, Amherst, MA, USA
- ¹⁰⁰ Department of Physics, McGill University, Montreal, QC, Canada
- ¹⁰¹ School of Physics, University of Melbourne, Melbourne, VIC, Australia
- ¹⁰² Department of Physics, University of Michigan, Ann Arbor, MI, USA
- ¹⁰³ Department of Physics and Astronomy, Michigan State University, East Lansing, MI, USA
- ¹⁰⁴ B.I. Stepanov Institute of Physics, National Academy of Sciences of Belarus, Minsk, Belarus
- ¹⁰⁵ Research Institute for Nuclear Problems of Byelorussian State University, Minsk, Belarus
- ¹⁰⁶ Group of Particle Physics, University of Montreal, Montreal, QC, Canada
- ¹⁰⁷ P.N. Lebedev Physical Institute of the Russian Academy of Sciences, Moscow, Russia
- ¹⁰⁸ National Research Nuclear University MEPhI, Moscow, Russia
- ¹⁰⁹ D.V. Skobel'syn Institute of Nuclear Physics, M.V. Lomonosov Moscow State University, Moscow, Russia
- ¹¹⁰ Fakultät für Physik, Ludwig-Maximilians-Universität München, Munich, Germany
- ¹¹¹ Max-Planck-Institut für Physik (Werner-Heisenberg-Institut), Munich, Germany
- ¹¹² Graduate School of Science and Kobayashi-Maskawa Institute, Nagoya University, Nagoya, Japan
- ¹¹³ Department of Physics and Astronomy, University of New Mexico, Albuquerque, NM, USA
- ¹¹⁴ Institute for Mathematics, Astrophysics and Particle Physics, Radboud University/Nikhef, Nijmegen, The Netherlands
- ¹¹⁵ Nikhef National Institute for Subatomic Physics and University of Amsterdam, Amsterdam, The Netherlands
- ¹¹⁶ Department of Physics, Northern Illinois University, DeKalb, IL, USA
- ¹¹⁷ ^(a)Budker Institute of Nuclear Physics and NSU, SB RAS, Novosibirsk, Russia; ^(b)Novosibirsk State University, Novosibirsk, Russia
- ¹¹⁸ Institute for High Energy Physics of the National Research Centre Kurchatov Institute, Protvino, Russia
- ¹¹⁹ Institute for Theoretical and Experimental Physics named by A.I. Alikhanov of National Research Centre “Kurchatov Institute”, Moscow, Russia
- ¹²⁰ Department of Physics, New York University, New York, NY, USA
- ¹²¹ Ochanomizu University, Otsuka, Bunkyo-ku, Tokyo, Japan
- ¹²² Ohio State University, Columbus, OH, USA
- ¹²³ Homer L. Dodge Department of Physics and Astronomy, University of Oklahoma, Norman, OK, USA
- ¹²⁴ Department of Physics, Oklahoma State University, Stillwater, OK, USA
- ¹²⁵ Joint Laboratory of Optics, Palacký University, Olomouc, Czech Republic
- ¹²⁶ Institute for Fundamental Science, University of Oregon, Eugene, OR, USA
- ¹²⁷ Graduate School of Science, Osaka University, Osaka, Japan
- ¹²⁸ Department of Physics, University of Oslo, Oslo, Norway
- ¹²⁹ Department of Physics, Oxford University, Oxford, UK
- ¹³⁰ LPNHE, Sorbonne Université, Université de Paris, CNRS/IN2P3, Paris, France
- ¹³¹ Department of Physics, University of Pennsylvania, Philadelphia, PA, USA
- ¹³² Konstantinov Nuclear Physics Institute of National Research Centre “Kurchatov Institute”, PNPI, St. Petersburg, Russia
- ¹³³ Department of Physics and Astronomy, University of Pittsburgh, Pittsburgh, PA, USA
- ¹³⁴ ^(a)Laboratório de Instrumentação e Física Experimental de Partículas-LIP, Lisbon, Portugal; ^(b)Departamento de Física, Faculdade de Ciências, Universidade de Lisboa, Lisbon, Portugal; ^(c)Departamento de Física, Universidade de Coimbra, Coimbra, Portugal; ^(d)Centro de Física Nuclear da Universidade de Lisboa, Lisbon, Portugal; ^(e)Departamento de Física,

- Universidade do Minho, Braga, Portugal; ^(f)Departamento de Física Teórica y del Cosmos, Universidad de Granada, Granada, Spain; ^(g)Instituto Superior Técnico, Universidade de Lisboa, Lisbon, Portugal
- 135 Institute of Physics of the Czech Academy of Sciences, Prague, Czech Republic
- 136 Czech Technical University in Prague, Prague, Czech Republic
- 137 Faculty of Mathematics and Physics, Charles University, Prague, Czech Republic
- 138 Particle Physics Department, Rutherford Appleton Laboratory, Didcot, UK
- 139 IRFU, CEA, Université Paris-Saclay, Gif-sur-Yvette, France
- 140 Santa Cruz Institute for Particle Physics, University of California Santa Cruz, Santa Cruz, CA, USA
- 141 ^(a)Departamento de Física, Pontificia Universidad Católica de Chile, Santiago, Chile; ^(b)Millennium Institute for Subatomic Physics at High Energy Frontier (SAPHIR), Santiago, Chile; ^(c)Universidad de la Serena, La Serena, Chile; ^(d)Department of Physics, Universidad Andres Bello, Santiago, Chile; ^(e)Instituto de Alta Investigación, Universidad de Tarapacá, Arica, Chile; ^(f)Departamento de Física, Universidad Técnica Federico Santa María, Valparaíso, Chile
- 142 Universidade Federal de São João del Rei (UFSJ), São João del Rei, Brazil
- 143 Department of Physics, University of Washington, Seattle, WA, USA
- 144 Department of Physics and Astronomy, University of Sheffield, Sheffield, UK
- 145 Department of Physics, Shinshu University, Nagano, Japan
- 146 Department Physik, Universität Siegen, Siegen, Germany
- 147 Department of Physics, Simon Fraser University, Burnaby, BC, Canada
- 148 SLAC National Accelerator Laboratory, Stanford, CA, USA
- 149 Department of Physics, Royal Institute of Technology, Stockholm, Sweden
- 150 Departments of Physics and Astronomy, Stony Brook University, Stony Brook, NY, USA
- 151 Department of Physics and Astronomy, University of Sussex, Brighton, UK
- 152 School of Physics, University of Sydney, Sydney, Australia
- 153 Institute of Physics, Academia Sinica, Taipei, Taiwan
- 154 ^(a)E. Andronikashvili Institute of Physics, Iv. Javakhishvili Tbilisi State University, Tbilisi, Georgia; ^(b)High Energy Physics Institute, Tbilisi State University, Tbilisi, Georgia
- 155 Department of Physics, Technion, Israel Institute of Technology, Haifa, Israel
- 156 Raymond and Beverly Sackler School of Physics and Astronomy, Tel Aviv University, Tel Aviv, Israel
- 157 Department of Physics, Aristotle University of Thessaloniki, Thessaloníki, Greece
- 158 International Center for Elementary Particle Physics and Department of Physics, University of Tokyo, Tokyo, Japan
- 159 Department of Physics, Tokyo Institute of Technology, Tokyo, Japan
- 160 Tomsk State University, Tomsk, Russia
- 161 Department of Physics, University of Toronto, Toronto, ON, Canada
- 162 ^(a)TRIUMF, Vancouver, BC, Canada; ^(b)Department of Physics and Astronomy, York University, Toronto, ON, Canada
- 163 Division of Physics and Tomonaga Center for the History of the Universe, Faculty of Pure and Applied Sciences, University of Tsukuba, Tsukuba, Japan
- 164 Department of Physics and Astronomy, Tufts University, Medford, MA, USA
- 165 Department of Physics and Astronomy, University of California Irvine, Irvine, CA, USA
- 166 Department of Physics and Astronomy, University of Uppsala, Uppsala, Sweden
- 167 Department of Physics, University of Illinois, Urbana, IL, USA
- 168 Instituto de Física Corpuscular (IFIC), Centro Mixto Universidad de Valencia-CSIC, Valencia, Spain
- 169 Department of Physics, University of British Columbia, Vancouver, BC, Canada
- 170 Department of Physics and Astronomy, University of Victoria, Victoria, BC, Canada
- 171 Fakultät für Physik und Astronomie, Julius-Maximilians-Universität Würzburg, Würzburg, Germany
- 172 Department of Physics, University of Warwick, Coventry, UK
- 173 Waseda University, Tokyo, Japan
- 174 Department of Particle Physics and Astrophysics, Weizmann Institute of Science, Rehovot, Israel
- 175 Department of Physics, University of Wisconsin, Madison, WI, USA
- 176 Fakultät für Mathematik und Naturwissenschaften, Fachgruppe Physik, Bergische Universität Wuppertal, Wuppertal, Germany
- 177 Department of Physics, Yale University, New Haven, CT, USA

^a Also at Borough of Manhattan Community College, City University of New York, New York, NY, USA

- ^b Also at Bruno Kessler Foundation, Trento, Italy
- ^c Also at Center for High Energy Physics, Peking University, Beijing, China
- ^d Also at Centro Studi e Ricerche Enrico Fermi, Rome, Italy
- ^e Also at CERN, Geneva, Switzerland
- ^f Also at Département de Physique Nucléaire et Corpusculaire, Université de Genève, Geneva, Switzerland
- ^g Also at Departament de Física de la Universitat Autònoma de Barcelona, Barcelona, Spain
- ^h Also at Department of Financial and Management Engineering, University of the Aegean, Chios, Greece
- ⁱ Also at Department of Physics and Astronomy, Michigan State University, East Lansing, MI, USA
- ^j Also at Department of Physics and Astronomy, University of Louisville, Louisville, KY, USA
- ^k Also at Department of Physics, Ben Gurion University of the Negev, Beersheba, Israel
- ^l Also at Department of Physics, California State University, East Bay, USA
- ^m Also at Department of Physics, California State University, Fresno, USA
- ⁿ Also at Department of Physics, California State University, Sacramento, USA
- ^o Also at Department of Physics, King's College London, London, UK
- ^p Also at Department of Physics, St. Petersburg State Polytechnical University, St. Petersburg, Russia
- ^q Also at Department of Physics, University of Fribourg, Fribourg, Switzerland
- ^r Also at Faculty of Physics, M.V. Lomonosov Moscow State University, Moscow, Russia
- ^s Also at Faculty of Physics, Sofia University, 'St. Kliment Ohridski', Sofia, Bulgaria
- ^t Also at Graduate School of Science, Osaka University, Osaka, Japan
- ^u Also at Hellenic Open University, Patras, Greece
- ^v Also at Institutio Catalana de Recerca i Estudis Avancats, ICREA, Barcelona, Spain
- ^w Also at Institut für Experimentalphysik, Universität Hamburg, Hamburg, Germany
- ^x Also at Institute for Particle and Nuclear Physics, Wigner Research Centre for Physics, Budapest, Hungary
- ^y Also at Institute of Particle Physics (IPP), Victoria, Canada
- ^z Also at Institute of Physics, Azerbaijan Academy of Sciences, Baku, Azerbaijan
- ^{aa} Also at Institute of Theoretical Physics, Ilia State University, Tbilisi, Georgia
- ^{ab} Also at Instituto de Física Teórica, IFT-UAM/CSIC, Madrid, Spain
- ^{ac} Also at Department of Physics, Istanbul University, Istanbul, Turkey
- ^{ad} Also at Joint Institute for Nuclear Research, Dubna, Russia
- ^{ae} Also at Moscow Institute of Physics and Technology State University, Dolgoprudny, Russia
- ^{af} Also at National Research Nuclear University MEPhI, Moscow, Russia
- ^{ag} Also at Physikalisches Institut, Albert-Ludwigs-Universität Freiburg, Freiburg, Germany
- ^{ah} Also at The City College of New York, New York, NY, USA
- ^{ai} Also at TRIUMF, Vancouver, BC, Canada
- ^{aj} Also at Università di Napoli Parthenope, Naples, Italy
- ^{ak} Also at University of Chinese Academy of Sciences (UCAS), Beijing, China
- ^{al} Also at Physics Department, Yeditepe University, Istanbul, Turkey
- * Deceased